STRUCTURE-PROPERTY RELATIONSHIP IN UREA-FORMALDEHYDE RESINS: EFFECT OF METHYLENE/ETHER BRIDGE RATIO AND ALKYL-SUBSTITUTED UREA CONTENT ON THE PERFORMANCE OF WOOD COMPOSITES

by
S. M. Ashik Abedin

Submitted to the Graduate School of Engineering and Natural Sciences
in partial fulfillment of
the requirements for the degree of Master of Science

SABANCI UNIVERSITY
July 2025

STRUCTURE-PROPERTY RELATIONSHIP IN UREA-FORMALDEHYDE RESINS: EFFECT OF METHYLENE/ETHER BRIDGE RATIO AND ALKYL-SUBSTITUTED UREA CONTENT ON THE PERFORMANCE OF WOOD COMPOSITES

APPROVED BY:

Assoc. Prof. Dr. Bekir Dizman ....
(Thesis Supervisor)

Prof. Dr. Yusuf Ziya Menceloğlu ....

Prof. Dr. Duygu Avcı Semiz ....

DATE OF APPROVAL: 03/07/2025

ABSTRACT

STRUCTURE-PROPERTY RELATIONSHIP IN UREA-FORMALDEHYDE RESINS: EFFECT OF METHYLENE/ETHER BRIDGE RATIO AND ALKYL-SUBSTITUTED UREA CONTENT ON THE PERFORMANCE OF WOOD COMPOSITES

S. M. Ashik Abedin

Materials Science and Nano Engineering MSc. Thesis, July 2025

Thesis Supervisor: Assoc. Prof. Dr. Bekir Dizman

Keywords: Modification of urea-formaldehyde resin, formaldehyde emission, wood composites, methylene and ether bridge, urea model compounds.

In recent decades, wood-based composite materials, owing to their global sustainability advantages and good surface hardness and dimensional properties, have been utilized in various fields, such as structural applications (construction and architecture), industrial applications (molds and pallets), furniture, and interior design. Wood composites are fabricated by combining and compressing lignocellulosic wood fibers or particles with a suitable resin or binder using a hot press system. Urea-formaldehyde (UF) resin is one of the most popular binders for fabricating wood-based composites, including particleboard and medium-density fiberboard, because of its easy production, low cost, good adhesion properties, and flexibility in the curing process. Although there are several benefits of using UF resin in fabricating wood composites, UF resin-based wood composites exhibit low moisture resistance and formaldehyde emission. Due to their low moisture resistance, UF-bonded wood composites cannot be used in outdoor environments. The gradual formaldehyde emission from the wood composites, attributable to the reversibility of condensation reactions of the UF resin, makes the widespread utilization of UF-bonded wood composites more challenging. Therefore, strategic modifications to its synthesis and crosslinking structure are essential for improving performance, an area that remains underexplored and warrants further research.

In this thesis, eight different UF resin synthesis processes were conducted to investigate the effects of changing the pH, time, temperature, and order of urea and formaldehyde addition on the structure of the UF resin. The methylene and the ether bridge ratio that define the final crosslinking structure were calculated for all synthesis procedures. Additionally, alkyl-substituted urea model compounds (1,1-dimethylurea and 1,3-dimethylurea) were incorporated with the UF resin at 5% and 10% of the original urea. In the first chapter, an introduction was provided to the background and development of UF resin and wood composites, as well as the detailed mechanism of the UF reaction and some modification strategies already explored in the literature. In the second chapter, one UF and one melamine urea formaldehyde (MUF) resin synthesis process were established as reference systems and comprehensively characterized using FTIR, NMR, DSC, and Rheology tests. Then, seven different UF synthesis processes were described, and each was specifically designed to enhance methylene bridge formation through systematic modification of reaction parameters. The methylene and ether bridge ratio was calculated using NMR spectroscopy, and the performance of board tests was also analyzed. In the third chapter, the impact of the incorporation of urea model compound was evaluated in terms of methylene and ether bridge ratio and board performance tests. In the final chapter, the research results and implications were summarized.

ÖZET

ÜRE-FORMALDEHİT REÇİNELERİNDE YAPI-ÖZELLİK İLİŞKİLERİ: METİLEN/ETER KÖPRÜSÜ ORANI VE ALKİL-SUBSTİTÜE ÜRE İÇERİĞİNİN AHŞAP KOMPOZİT PERFORMANSI ÜZERİNDEKİ ETKİSİ

S. M. Ashik Abedin

MALZEME BİLİMİ VE NANO MÜHENDİSLİK, Yüksek Lisans Tezi, Temmuz 2025

Tez Danışmanı: Doç. Dr. Bekir Dizman

Anahtar Kelimeler: Üre-formaldehit reçinesinin modifikasyonu, formaldehit emisyonu, ahşap kompozitler, metilen ve eter köprüsü, üre model bileşikleri.

Son yıllarda, küresel sürdürülebilirlik avantajları ile iyi yüzey sertliği ve boyutsal kararlılık özellikleri sayesinde, ahşap esaslı kompozit malzemeler; yapısal uygulamalar (inşaat ve mimarlık), endüstriyel uygulamalar (kalıplar ve paletler), mobilya ve iç mekân tasarımı gibi çeşitli alanlarda yaygın olarak kullanılmaktadır. Bu kompozitler, lignoselülozik ahşap lifleri veya parçacıklarının uygun bir reçine veya bağlayıcı ile birleştirilip sıcak pres sistemi ile sıkıştırılmasıyla üretilmektedir. Üre-formaldehit (UF) reçinesi; kolay üretimi, düşük maliyeti, iyi yapışma özellikleri ve kürlenme sürecindeki esnekliği nedeniyle, yonga levha ve orta yoğunluklu lif levha (MDF) gibi ahşap esaslı kompozitlerin üretiminde en yaygın kullanılan bağlayıcılardan biridir. UF reçinesinin ahşap kompozit üretiminde kullanımının çeşitli avantajları bulunmakla birlikte, bu reçineye dayalı kompozitler düşük nem direnci ve formaldehit emisyonu gibi önemli dezavantajlara sahiptir. Düşük nem direnci nedeniyle UF reçinesi ile bağlanmış ahşap kompozitler dış ortam koşullarında kullanılamamakta, ayrıca UF reçinesinin kondenzasyon reaksiyonlarının geri dönüşümlü doğası nedeniyle zamanla formaldehit salımı gerçekleşmektedir. Bu durum, UF esaslı kompozitlerin yaygın kullanımını önemli ölçüde kısıtlamaktadır. Bu bağlamda, UF reaksiyon mekanizmasının ve ara ürün oluşum koşullarının kapsamlı bir şekilde anlaşılması ile birlikte, reçine sentez sürecinin ve çapraz bağ yapısının modifikasyonu, söz konusu problemlerin giderilmesi açısından büyük önem taşımaktadır. Bu özel yaklaşım, bugüne kadar literatürde derinlemesine incelenmemiş olup, ileri düzeyde bilimsel araştırmalar için önemli bir fırsat sunmaktadır.

Bu tez kapsamında, pH, süre, sıcaklık ve üre ile formaldehitin eklenme sırasının UF reçinesinin yapısına etkilerini araştırmak amacıyla sekiz farklı UF reçine sentezi gerçekleştirilmiştir. Nihai çapraz bağ yapısını tanımlayan metilen ve eter köprüsü oranları, tüm sentez işlemleri için hesaplanmıştır. Ayrıca, alkil-substitüe üre model bileşikleri (1,1-dimetilüre ve 1,3-dimetilüre), orijinal ürenin %5 ve %10'u oranında UF reçinesine dâhil edilmiştir. Birinci bölümde, UF reçinesi ve ahşap kompozitlerin geçmişi ve gelişimi, UF reaksiyonunun detaylı mekanizması ve literatürde daha önce incelenmiş bazı modifikasyon stratejileri sunulmuştur. İkinci bölümde, bir UF ve bir melamin-üre-formaldehit (MUF) reçine sentezi referans sistem olarak belirlenmiş ve bu sistemler FTIR, NMR, DSC ve Reoloji analizleriyle kapsamlı bir şekilde karakterize edilmiştir. Ardından, metilen köprüsü oluşumunu artırmaya yönelik olarak reaksiyon parametrelerinin sistematik modifikasyonu ile tasarlanan sekiz farklı UF sentez yöntemi detaylı olarak açıklanmıştır. Metilen ve eter köprüsü oranları NMR spektroskopisi ile hesaplanmış ve levha performans testleri değerlendirilmiştir. Üçüncü bölümde, üre model bileşiklerinin reçine sistemine katılmasının metilen ve eter köprüsü oranlarına ve levha performansına etkisi analiz edilmiştir. Son bölümde ise araştırma sonuçları ve bu sonuçların olası etkileri özetlenmiştir.

ACKNOWLEDGEMENTS

I want to express my sincere gratitude to my thesis advisor, Assoc. Prof. Dr. Bekir Dizman. I am honored to be one of his students, and I want to thank him for his guidance, support, and encouragement during this master's thesis. I want to thank the thesis jury members, Prof. Dr. Yusuf Ziya Menceloğlu and Prof. Dr. Duygu Avcı Semiz, for their valuable time, critical evaluation, and constructive comments.

I would like to thank Nur Gumus and Kamile Ertaş Işık for being such perfect teammates. As a team of three, we managed to progress our studies successfully in the laboratory. I know that we have a friendship that will last for many years. I want to thank Aylin Yıldırım Özel for her motivation and different advice during these two years. I especially would like to thank Saeed Salamatgharamaleki for his unconditional help whenever I needed him during the research. Besides working in labs, my special thanks go to him for giving me the chance to be his friend. I am also grateful for his support in processing and presenting the data.

I am also thankful to my friends Cuma Ali Ucar, Negar Amirhaghian, Ece Şahin, Mehmet Sinan Tübcil, Ceren Özsaltık, and Büşra Amanvermez for their kind support throughout the work.

I would like to express my gratitude to the Department of R&D, Kastamonu Integrated Wood Industry, Sabanci University, and SU-IMC members, especially Turgay Gönül, Yaşar Güray, Burak Özdemir, Erdal Balcı, and Şevki Sark, for providing amazing lab environments and their technical support.

Special thanks to my parents for their invaluable support during my education.

This project is funded by the Scientific and Technological Research Council of Turkey (TUBITAK) under grant number 5230047.

Dedicated to my beloved parents for their unconditional love and support

TABLE OF CONTENTS

LIST OF FIGURES

LIST OF TABLES

LIST OF ABBREVIATIONS

DMU: Dimethyl Urea

DMUF: Dimethyl Urea Formaldehyde

F/U: Formaldehyde to Urea ratio

IB: Internal Bond

MDF: Medium-Density Fiberboard

MUF: Melamine-Urea-Formaldehyde

PB: Particleboard

UF: Urea-Formaldehyde

WHO: World Health Organization

1 Introduction

1.1 Historical Development of UF Resin

Urea-formaldehyde (UF) resin is one of the most popular amino plastic resins and has extensive applications in interior wood composite products, including particleboard (PB) and medium-density fiberboard (MDF), due to its low production cost (initially good water solubility), good internal bond (IB) strength, absence of color in cured polymers, and flexibility in curing process [1, 2]. The UF resin represents 80% of total amino resin production over the world, and 68% of it is utilized for manufacturing PB and MDF and around 22% is used for plywood production [3]. Although the UF resin synthesis includes two monomers, urea and formaldehyde, it is a complex multistep reaction that depends on the reaction conditions not only for the reaction rate but also for the properties of the final products, which ultimately lead to both linear and branched polymers and a three-dimensional crosslinking network at the curing stage [2]. Without understanding the polymerization process completely, UF resin was first synthesized in 1884 by Holzer and Tollens [4]. Since the initial discovery in the early 1880s that the reaction between urea and formaldehyde yields a resinous substance, the development of UF resins has undergone significant evolution [5]. In 1887, two patents were published by Goldschmidt and John, which furthered understanding of the reaction and initiated the commercialization of UF resin [6-8]. Following this, between 1930 and 1950, different formaldehyde-based resins were synthesized and commercially produced, including phenol–formaldehyde, melamine-urea formaldehyde (MUF), and melamine formaldehyde(MF) [8]. In the early stages of commercialization, UF resins were relatively costly and primarily utilized as molding materials [5]. Since their initial development, the applications of UF resins have undergone significant transformation. The primary use has shifted from molding compounds to adhesive formulations, particularly in the production of wood-based composites. This shift in end-use, accompanied by increased global consumption, has driven substantial advancements in the underlying resin chemistry to meet evolving performance and processing requirements [5]. Despite the long history of commercial UF resin synthesis, the kinetics of this complex reaction system is not comprehensively understood yet [5, 9, 10].

1.2 Background and Significance of Wood Composites

Over the past 40 years, PB and MDF have been among the most widely utilized engineered wood composites in furniture manufacturing, structural applications, and interior decoration, with an annual production of millions of tons [11]. Their popularity is attributed to their desirable surface hardness, good mechanical properties, and versatility in structural applications. The commercialization of wood composites began with veneer-based products like Impreg and Compreg, followed by radiation-cured and heat-catalyst-cured lumber-based wood composites [12]. Since the 1950s, North America has seen the rapid adoption of both structural and non-structural wood composites, often substituting for traditional solid wood products [13]. The wood-plastic composites industry in the United States has experienced significant growth since the mid-1990s, attracting interest from both the plastics and forest products sectors [14]. This growth is driven by changing social and economic trends, which have increased pressure on the forest products industry to improve product performance and implement environmentally friendly technologies [13, 14]. Wood composites are manufactured by combining lignocellulosic wood fibers or particles with a suitable resin or a suitable binder to form a composite material [11]. A solid board is produced by compressing the lignocellulosic wood particles and resin with a hot press system. Both the quality of the wood particles and the resin contribute to the final properties of the wood composites. Both PB and MDF are primarily manufactured from wood-based residues or other forms of industrial wood waste, thereby promoting efficient resource upcycling and environmental sustainability [15]. Due to their wood-based composition, both PB and MDF are inherently susceptible to water, moisture, and humidity [11, 16]. However, recently, there have been some innovations in the wood composites sector that offer biobased and moisture-resistant, fire-retardant products that catch attention for high-end use [17, 18]. UF and melamine-urea-formaldehyde (MUF) are the two predominant amino resins for producing wood-based composites due to several factors, including the low cost, better compatibility, acceptable formaldehyde emissions, low formaldehyde content, and desirable mechanical properties [18-20]. UF resin is mostly used for interior products due to its low moisture resistance, while MUF is preferable for outdoor applications as MUF exhibits better resistance to moisture and lower susceptibility to hydrolysis [19]. In some manufacturing processes, phenol formaldehyde resin is also used at very low proportions with MUF, which requires higher curing temperature, mainly for niche products [19]. In recent years, some bio-based resins (from natural resources) such as soy-based adhesives and lignin- and tannin-based adhesives have also been utilized for producing wood composites, considering environmental safety and sustainability [21-24]. However, in general, composites produced with biobased resins show inferior mechanical properties compared to standard petrochemical-based composites. The demand for recyclable, environmentally sustainable, and cost-effective composite materials is increasing day by day. In this context, wood composites have garnered significant attention from researchers due to their eco-friendly nature, low production cost, which is attributable to the use of waste wood particles [15].

1.3 Chemistry of Urea and Formaldehyde

1.3.1 Formaldehyde

Formaldehyde is a highly versatile monomeric precursor extensively utilized in the synthesis of polymeric materials, including resins, thermosets, and engineering plastics, due to its high reactivity and functionality in polymerization and crosslinking reactions. Formaldehyde, a widely used chemical with both industrial and biological significance, exhibits complex chemistry in its interactions with biological molecules. It reacts efficiently with amino acids, particularly cysteine, forming stable products like thiazolidines [25]. In protein chemistry, formaldehyde is utilized for crosslinking studies, enabling the analysis of chromatin complexes and protein-DNA interactions [25, 26]. The compound's reactivity extends to coordination chemistry, where it forms stable complexes with metals like iridium, demonstrating potential for CO reduction processes [27]. The aqueous solution of formaldehyde (30% to 50%) is known as formalin, where formaldehyde predominately stays in its monomeric hydrate, methylene glycol [28] (**Figure 1**).

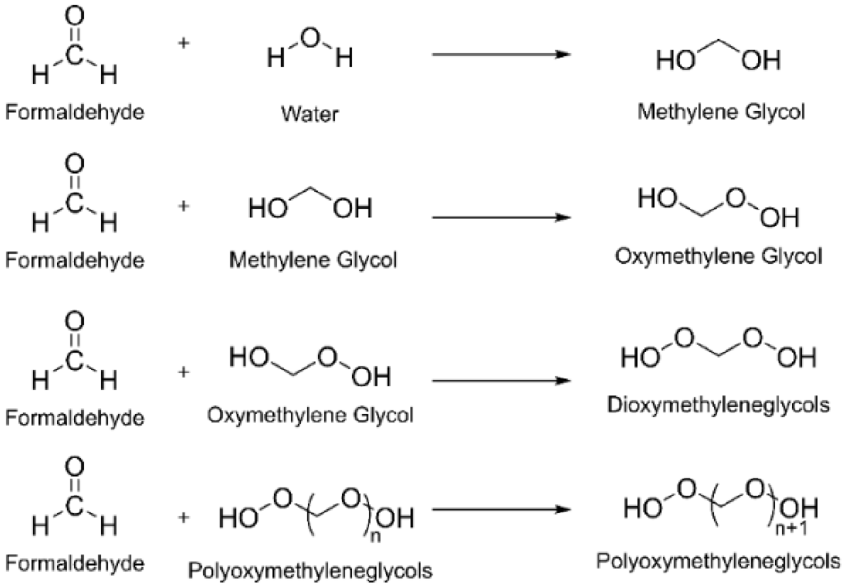

Figure 1. Formaldehyde in water

Formaldehyde water system exhibits complex physicochemical properties and interactions. Car-Parrinello simulations have shown that formaldehyde's n → π* excitation energy experiences a blue shift when transitioning from gas to aqueous phase, and a thermodynamic model was established by Albert et al. [29, 30].

Methanol and various amine derivatives are usually added to the solutions as stabilizers to reduce intrinsic polymerization, and commercially available formaldehyde-alcohol solutions are stable [28]. Formaldehyde is very soluble in water, ethanol, and diethyl ether. Formaldehyde is a widespread xenobiotic air pollutant with significant toxic effects on human health, particularly through occupational exposure [31]. It causes deleterious effects on various organs, including the lungs, upper respiratory tract, bone marrow, and brain [31]. Formaldehyde exposure leads to inflammation, oxidative stress, and genotoxicity in both humans and animals [31].

1.3.2 Urea

Urea (known as carbonic acid diamide or carbamide) is an odorless, colorless, solid crystalline compound (due to sp^2 hybridization of the N orbitals) with a melting point of 133°C [32]. It is highly soluble in water and ethanol. Urea is recognized as the first organic compound synthesized in a laboratory environment and a pioneer compound in modern organic synthetic chemistry. In 1773, urea was first discovered in urine by Rouelle, and in 1828 first synthesized from ammonia and cyanic acid by the German chemist Friedrich Wöhler, the founding father of synthetic organic chemistry [33]. In recent years, urea derivatives have gained significant attention in organic chemistry due to their versatile applications. These compounds have emerged as valuable tools, serving not only as hydrogen-bond donors in organocatalysis and anion transport systems but also as key frameworks in supramolecular design [34]. Additionally, they play crucial roles in directing lithiation processes, acting as amination substrates, facilitating metalation reactions, and serving as intermediates in novel rearrangement transformations [34]. Due to the planar structure of the urea linkage, all four N substituents are precise and organized. Urea has become an ideal compound for catalyst structures due to its ability to bind carbonyl groups selectively in a precise orientation [34]. The main uses of urea are in agriculture as a fertilizer. The cosmetics industry utilizes urea for its solubility and moisturizing properties [35]. In medicinal chemistry, urea-containing compounds are being employed to establish key drug-target interactions and optimize drug-like properties [36]. Urea is also used in reducing NOx emissions by catalytic reduction [37].

In commercial production, to synthesize urea, first, ammonium carbamate is formed by the direct reaction of ammonia (ammonia is formed through the reaction of nitrogen and hydrogen) and carbon dioxide. Then, ammonium carbamate is dehydrated at high temperatures and pressure to obtain urea [37]. Although yet to be commercialized, a groundbreaking research conducted by C. Chen et al. showed that urea synthesis by coupling of nitrogen and carbon dioxide in water is assisted by PdCu alloy nanoparticles under ambient settings [38]. Urea is generally recognized as a non-toxic compound [37].

1.4 The UF Reaction System

The UF resin synthesis reaction is a pH-dependent Mannich reaction [39]. In general, the reaction is conducted under mildly alkaline conditions to promote the formation of methylol groups, followed by acid-catalyzed condensation to advance polymerization. However, several other methods with two to four-step reactions for synthesizing UF resin have been reported in the literature through controlling the reaction parameters such as pH, temperature, formaldehyde to urea mole ratio, and changing the order of methylolation-condensation stage, based on the two main principle reactions, named methylolation and condensation [40]. The pH of the methylolation stage should not be higher than 9.0, as there is a possibility of Cannizarro side reaction that produces a substantial amount of methanol under strong basic conditions. The main product of the methylolation stage is the methylolureas (mono, di, and tri-hydroxymethyl ureas are the most expected, but tetrahydroxymethylurea and oxymethylene groups may also be formed), and at the condensation stage, the methylolureas react further with urea and unreacted formaldehyde and form mainly methylene and methylene ether bridges, and may form cyclic bridges [41, 42]. The stable methylol carbonium ion is formed through intramolecular proton transfer, assisting the formation of methylene and methylene ether bridges [43]. The reaction kinetics of UF resin have been extensively studied and reported in the literature [44-47]. The ratio of one, two, and three methylol groups is estimated at 9:3:1 [1]. The reaction rate of methylolation at a basic pH is much higher than that of condensation at an acidic pH [44, 45]. The reaction rate of UF is three times higher at a 1:1 (urea: formaldehyde) mole ratio than at the 1:2 mole ratio. The condensation reaction requires a pH lower than 7, and the reaction speed decreases exponentially from a pH of 2 to 3 to a pH of 7, and no reaction occurs at basic pH [1].

1.4.1 UF Reaction Kinetics

To improve the performance of the resin, reaction kinetics must be understood properly. Through the middle of the last century, the fundamental theory of UF reaction was established based on two reactions, first methylolation or addition, and second, condensation, which provides the basic information of the UF reaction kinetics [48]. However, those fundamental studies are not capable of describing this complex reaction system due to having multiple routes, competitive reactions, and changes in reaction with different parameters, including pH, time, temperature, and F/U. In recent times, to understand the reaction more closely, numerous studies have capitalized the use of modern analytical technology, such as NMR, Mass Spectrometry, and FTIR. UF reaction is a first-order reaction concerning the pH, ranging from 0.99 to 12.45 at 40ºC [49]. The reaction in general follows the Brønsted relationship, a linear free energy relationship (LFER) to the acidity and basicity constants of the catalyst [49]. At higher pH (above 11), the formation of methanol (Cannizzaro reaction) is competitive with the formation of methylol [49].

1.4.2 Mechanism of Methylolation (Addition)

The mechanism of methylolation is shown in **Figure 2**.

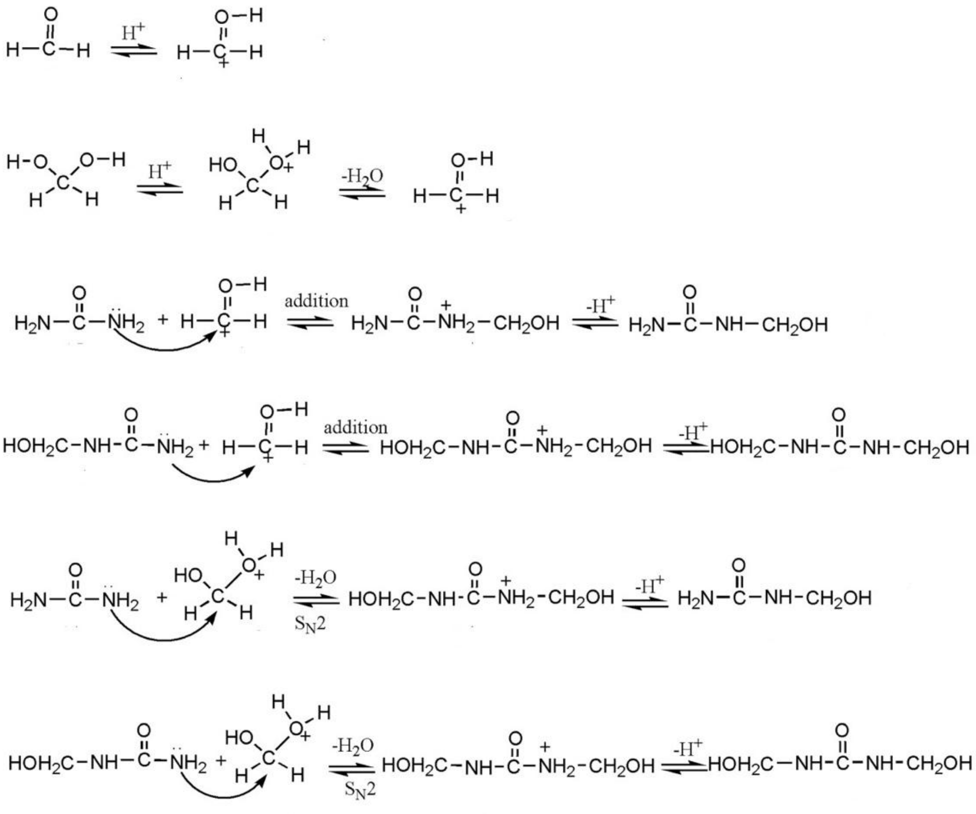

Figure 2. Reaction mechanism of the methylolation reaction

From the fundamental studies, it is well known that when formaldehyde is protonated, it is very reactive towards nucleophiles such as urea. This is evident from the reaction speed of UF catalyzed by acid compared to that catalyzed by bases or neutral conditions. A very stable hydrogen-bonding complex is formed with an energy of 101.3 kJ/mol, lower than the starting molecules [50]. Deprotonation of intermolecular forms neutral monomethylol urea, and the next addition between formaldehyde and monomethylol urea forms dimethylolurea.

1.4.3 Mechanism of Condensation

The mechanism of condensation is shown in **Figure 3**.

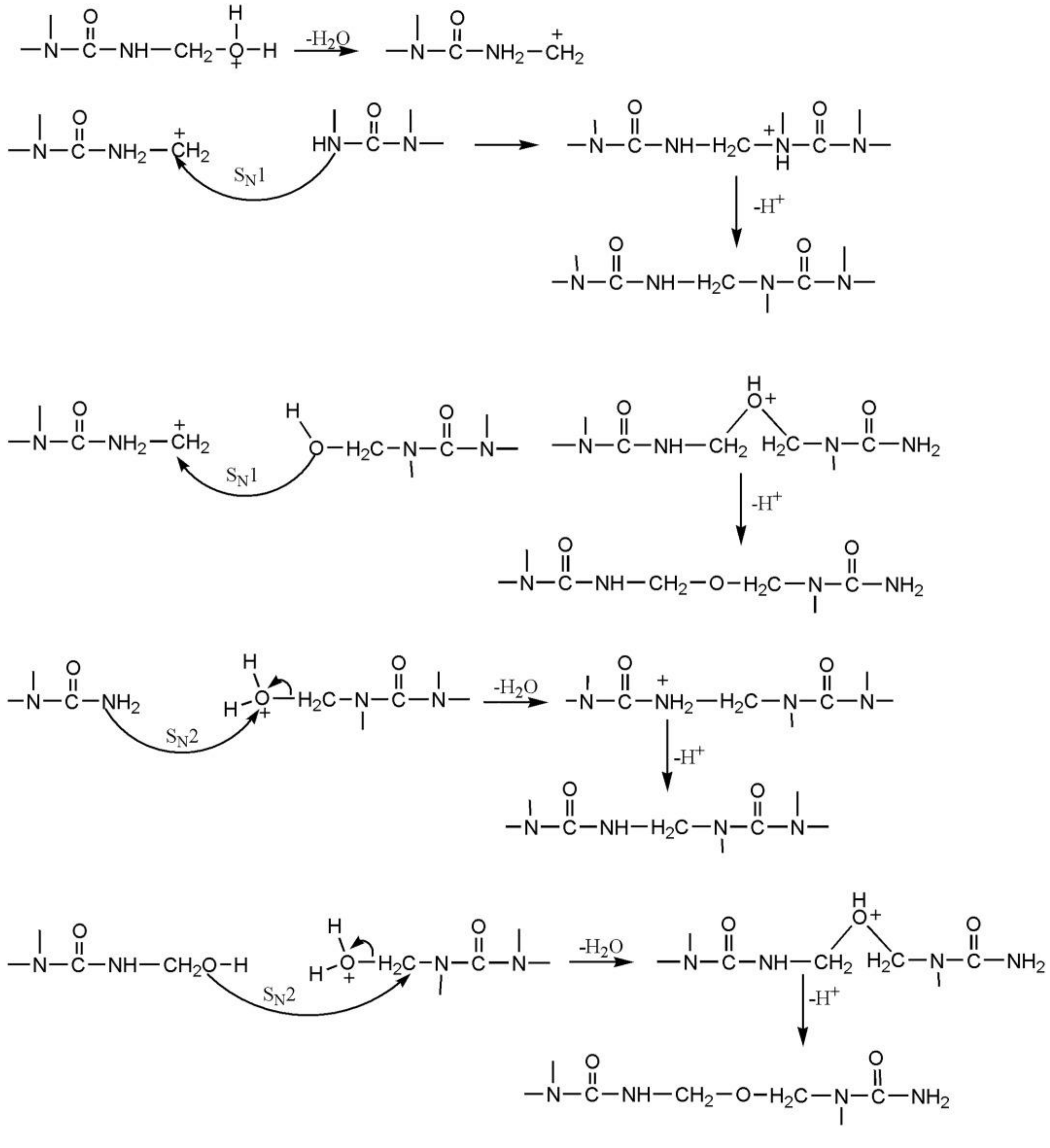

Figure 3. Mechanism of Condensation Reaction

Methylene and ether bridges are formed at this stage through the condensation of methylols with an acid catalyst. Methylol urea eliminates one water molecule. De Jong et al. and Sun et al. proposed that methylol groups are similar to biomolecular reactions, whereas Francis et al. proposed the formation of carbocation [48, 51, 52]. However, the proposal for the formation of carbocation is generally accepted due to its easy explanation through the conjugation effect [50].

1.4.4 Formation of Carbocation

The mechanism for the formation of carbocation is shown in **Figure 4**.

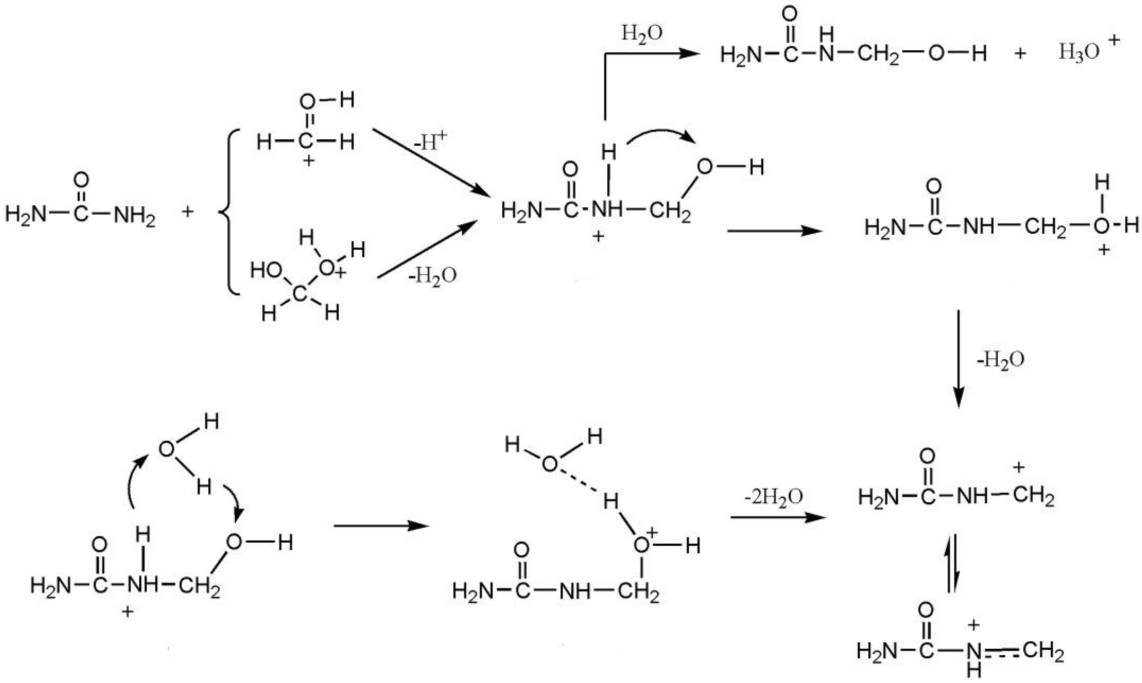

Figure 4. Mechanism of Carbocation Formation

De Jong et al. found that the formation of carbocation implies that the methylene bridge is more likely compared to the ether bridge, due to the unsubstituted $-NH_2$ of urea is highly reactive towards carbocation that ultimately forms the methylene bridge [53]. This phenomenon can be explained by the higher nucleophilicity of $-NH_2$ compared to the nucleophilicity of nitrogen or oxygen atoms present in the methylol reaction. The formation of the ether bridge is slower than the methylene bridge as it is evident from this mechanism [50, 53].

1.4.5 Reaction between Carbocation and Methylolureas

The methylene bridge is mainly formed through the reaction of carbocation and methylurea, which is thermodynamically more favorable compared to the ether bridge (**Figure 5**). The dimethylolurea carbocation can react with dimethylolurea to form a linear ether bridge or a branched methylene bridge, and the barrier for this reaction is very minimal [50]. The energy of the methylene bridge formed through this reaction is 66.0

kJ/mol, which is lower than the reactant species, ultimately making the methylene bridge more stable and thermodynamically favorable [50]. The methylene bridge formed through the reaction of dimethylolurea has a 27.7 kJ/mol higher barrier (attacking of -CH_2^+ on -OH during the transition state) compared to the formation of monomethylolurea. As a result, monomethylolurea is thermodynamically more favourable than the ether bridge formation [50]. However, steric hindrance can also play here in the formation of the methylene bridge along with the barrier energy. Taohong Li et al. concluded that the methylene bridge is thermodynamically favourable than the ether bridge, whether the reactant is dimethylolurea or monomethylolurea [50].

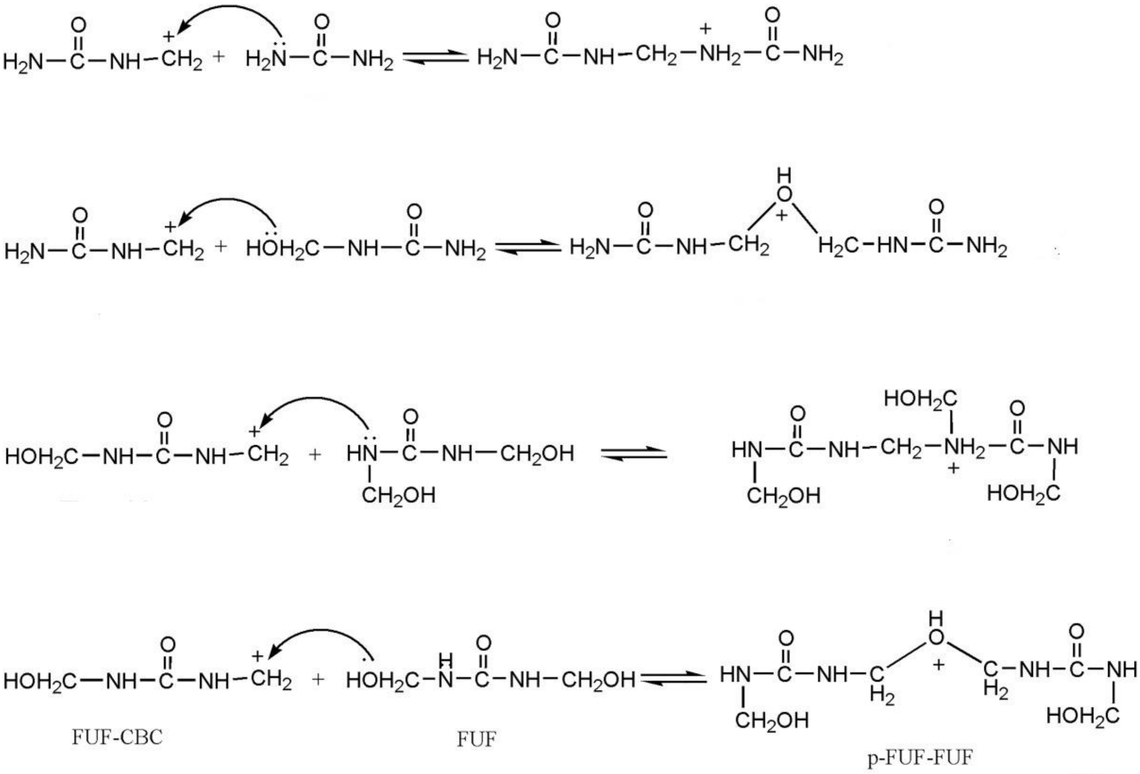

(10)

Figure 5. Reaction mechanism between carbocation and methylolurea: fundamentals of UF resin crosslinking

1.4.6 Crosslinking of UF: Methylene and Ether Bridges

The crosslinked structure of the UF resin is very complicated and changes rapidly with the change of reaction parameters [50]. It consists mostly of methylene and ether bridge, and in some cases, cyclic uron structure. The formation of methylene and methylene ether bridges is mostly dependent on pH, formaldehyde to urea ratio (F/U), and temperature of the reaction [2, 50]. Ether bridges are formed at basic pH and low temperature, whereas methylene bridges are formed at higher temperature and acidic pH, which is also consistent with the theoretical study showing lower energy barriers for methylene bridge formation in acidic conditions and ether bridge formation at basic conditions [2, 50].

1,1'-(oxybis(methylene))diurea

1,1'-methylenediurea

Figure 6. Crosslinking network of UF Resin: Formation of methylene and methylene ether bridge

Methylene bridges are comparatively more stable than the ether bridge; the ether bridge formed in the alkaline condition yields low crosslinking density and is not stable hydrolytically [2, 50]. The conversion or rearrangement of the ether bridge into a methylene bridge in the UF reaction system is also possible at very high temperatures and low pH, and has been a subject of extensive research [50]. Although the exact mechanism is not clear at this moment, the higher thermodynamic stability of the methylene bridge could be a possible reason [50]. The most accepted possible mechanism for the rearrangement of the ether bridge in the methylene bridge is given in **Figure 7** [50]. However, another possible mechanism also proposed by Taohong Li et al. is provided in **Figure 8** [50]. The addition of melamine to the UF reaction system substantially changes the methylene to ether bridge ratio, and it assists formation of more methylene bridges, as proven by A. Despres et al. through ^{13}C NMR and MALDI-TOF spectrometry [54]. Additionally, formaldehyde and urea do not show equal reactivity as expected from the functional group that impacts the reaction [55-57].

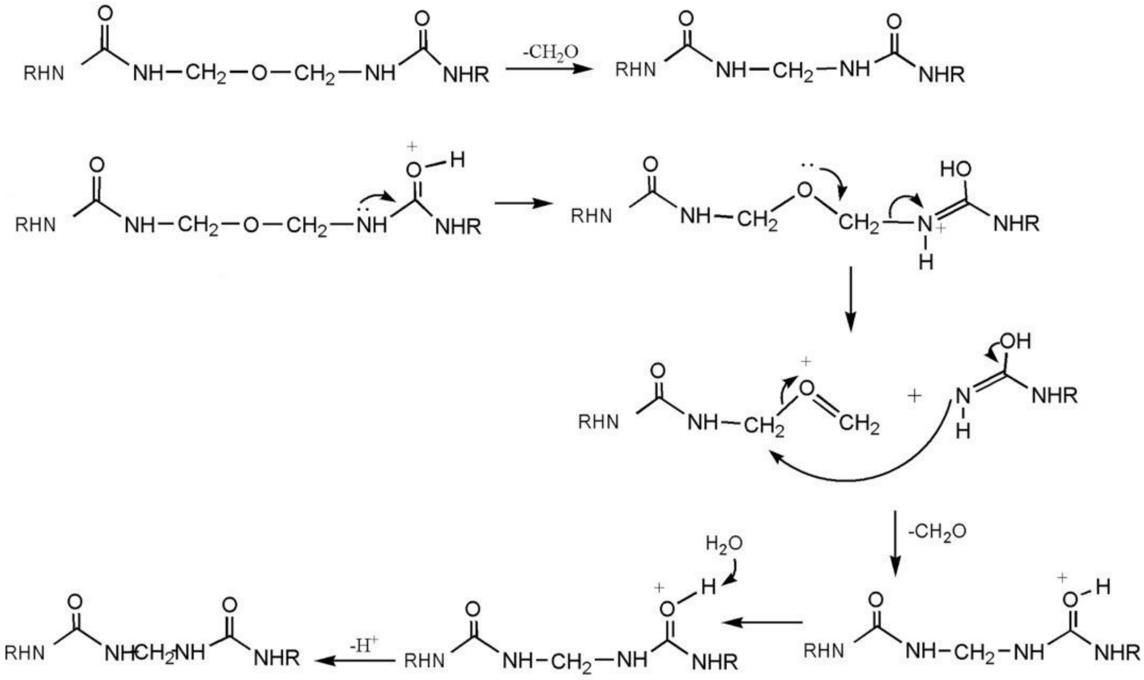

Figure 7. Mechanism 1 for the rearrangement of the ether bridge to the methylene bridge

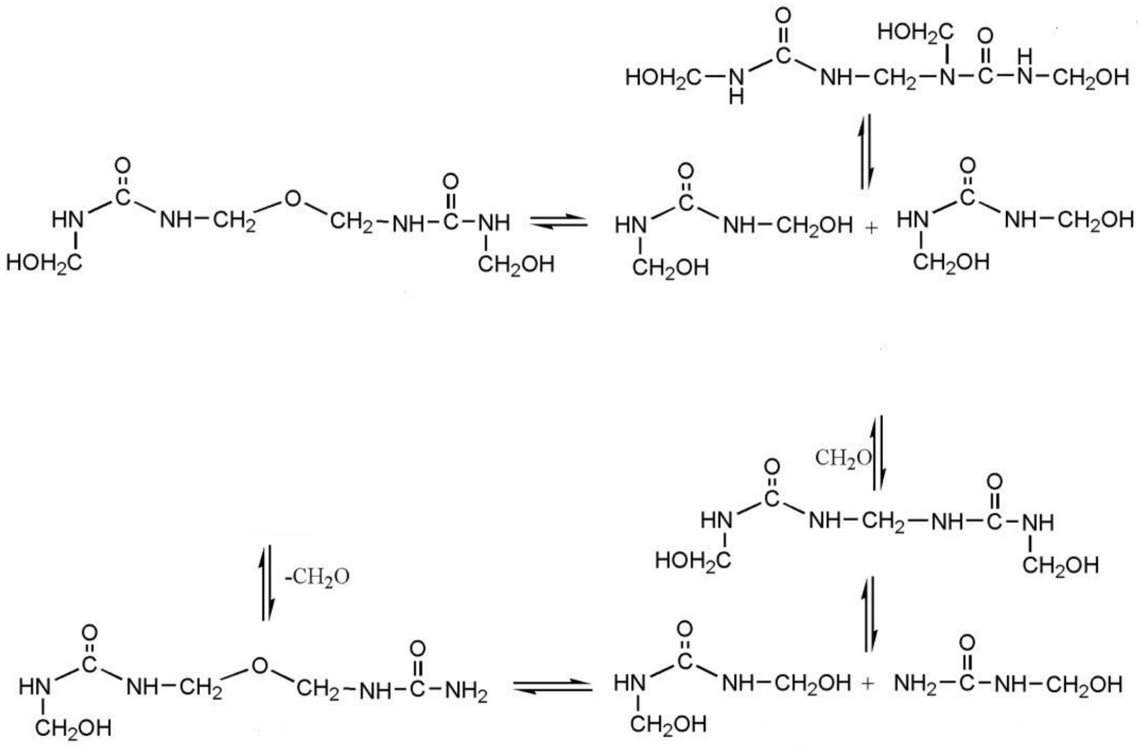

Figure 8. Mechanism 2 for the rearrangement of the ether bridge to the methylene bridge

Theoretical calculations of energy barriers and reaction mechanisms imply that the competitive formation of methylene and ether bridges is affected by the energy barriers of the UF reaction system and the steric hindrance effect [50]. The thermodynamic properties of the UF reaction system suggest that the methylene bridge is predominantly formed in the later stages of condensation [50]. Theoretically, the cyclic uron structure can also be formed at the condensation stage. However, this is very unlikely and formed very slowly under mild acidic conditions [50].

1.5 Limitations of Conventional UF Resin

UF resin is the most widely used adhesive system for the fabrication of wood-based composites. However, their processability and curing behavior are determined by a range of factors, including the intrinsic properties of the resin, the type and characteristics of the wood substrate, the nature and concentration of catalysts, the incorporation of other polymers, as well as environmental conditions. These factors collectively determine the manufacturability and performance of UF resin-based composites in applications such as plywood, particleboard, and fiberboard production. Although UF resin has several benefits, including low cost and ease of preparation, it poses concerns regarding formaldehyde emissions from the product over time and low resistance to moisture [1, 2, 5, 8]. Poor moisture resistance and high formaldehyde emissions are reported as the major drawbacks to using UF resin in outdoor environment products. The main reason for the formaldehyde emission is the reversibility of the reactions [2]. Both the methylolation and condensation reactions of the UF system are reversible and release formaldehyde during the reverse reactions [2]. The second reason is the low moisture resistance problem, which is mainly due to the hydrolysis of the chemical bonds in the polymer chain in outdoor environments [2]. Along with these two major problems, UF resin also shows brittleness. Due to the low press time in wood composites preparation, UF should be highly reactive and require a substantial amount of hardener, which may be incorporated in the network and release gradually later [2].

1.5.1 Environmental and Health Concerns

For humans, formaldehyde is considered a highly toxic material. Even at minimal amounts and regardless of the intake method, formaldehyde can cause severe damage to human organs and can cause cancer [58]. In 2006, the International Agency for Research on Cancer declared that formaldehyde would be classified as carcinogenic (Group 1) [59]. An investigation by the Wisconsin Division of Health suggests that formaldehyde release from the UF resin or wood products may cause several health problems, including eye irritation, headache, and a runny nose, based on 100 structures tested [60]. This study also suggests that formaldehyde emission is significant for nonoccupational indoor environments and may exceed occupational exposure guidelines [60]. According to the World Health Organization (WHO), formaldehyde can be released to the environment during the production, storage, transportation, and from residual formaldehyde in the system [61]. The higher formaldehyde emission from the UF resin is a major drawback for the widespread use of wood composites manufactured with UF resin. Regarding this severe health issue, formaldehyde emission from the UF resin needs to be addressed properly. In 1977, the German Federal Agency of Health, for the first time, limited the human exposure to formaldehyde to 0.1 ppm [61]. In 1981, Germany and Denmark, for the first time, established the limitations and regulations for formaldehyde emission in dwellings for wood-based panels [61]. There are different levels of standards set by the authorities in many countries, and the acceptance level of formaldehyde is lowered day by day, i. e., the current range is 0.05 ppm to 0.11 ppm set by the California Air Resources Board (CARB) regulation [62].

1.6 Modification Strategies for UF Resin

To address the limitations of using UF resin, several modifications and improvement are described in the literature. Lowering the F/U ratio is mentioned in numerous studies and is well established to reduce the formaldehyde emissions[1, 2]. However, lowering the F/U ratio reduces the crosslinking density of the UF structure and hence affects the mechanical properties of the wood composites [1, 2, 8, 15]. Modifying UF resins with alcohols, particularly n-butyl alcohol, can improve their properties [63]. Adding melamine to create MUF resins enhances heat and water resistance, though excessive melamine can decrease water resistance [64]. Additionally, using melamine in the UF reduces the storage ability of the resin due to the high reactivity of the melamine, and the high price of melamine also increases the overall production cost [2]. The buffering capability of the triazine ring of melamine increases the required amount of hardener [2]. Melamine acetates are also used in some cases, and those are dissolved at high temperatures and give better moisture resistance [1]. In some studies, phenol was also included in the UF resin synthesis with and without melamine and it was reported that incorporating the phenol increases moisture resistance. However, incorporation of phenol in the UF system reduces the reactivity of formaldehyde [2]. Branched polyurea-based UF resin performed better compared to the unmodified UF resin, considering the water resistance and formaldehyde emission, where polyurea was synthesized through the condensation of urea and tris (2-aminoethyl) amine [65]. Partial substitution of urea in the UF reaction has become a popular method for modifying the UF resin, improving water resistance, and reducing formaldehyde emission. Tannin was partially substituted for urea in the UF synthesis, providing a 39% reduction in formaldehyde emission and good water resistance in the internal bonding test [66]. Polyamine in the form of partially hydrolysed nylon can also be utilized in the UF reaction system, considering the tertiary amide can react with available methylol groups [1]. Keratin was also used to modify the UF resin to reduce the toxicity and overall cost through the copolymerization reaction [67]. To reduce the free formaldehyde and improve the mechanical properties of the UF resin, different types of fillers and modifiers were also used, such as cellulose nanofibrils, polydimethylsiloxane, N-butyl alcohol, flexible diamines and triamines, and dicyclohexylcarbodiimide [68, 69]. Amine hydrochlorides were also used as a curing agent to improve the UF resin properties [70]. In considering environmental sustainability, different bio-based resins were synthesized, such as natural polyphenols and protein-based resins, and applied as a replacement for UF resin [71]. However, those show very low adhesion performance, difficulty in large-scale production, and higher cost [71].

1.6.1 Incorporation of Alkyl-Substituted Urea Compounds

Due to the complexity of the UF reaction system, understanding the reaction progress in terms of qualitative and quantitative information is very difficult. The main reasons for this complexity are multiple paths of reaction, competitiveness between multiple reactions that are possible simultaneously, changes in the intermittent product with the change of reaction parameters, and large numbers of structurally similar or close products [1, 2, 45, 50, 51, 72]. Among them, due to having similar or close structures, those intermittent products show similar or close spectroscopic properties, and make the NMR analysis very complicated [72]. Along with UF's main reaction intermittence with the uncertainty on the number of substitutions on urea, formaldehyde can react with itself and homopolymerize, and the possibility of side reactions, including the Cannizzaro reaction, to form methanol, makes the entire system very complicated to analyze with the NMR technique. The most convenient way to control the reaction is to limit the number of available active sites of urea to react with formaldehyde [72]. In this context, 1,3-dimethylurea (1,3 DMU) and 1,1-dimethylurea (1,1 DMU) can serve as model compounds for urea in the reaction due to their similar structure, intermolecular mobility, and molecular size. The substitution of methyl groups in the urea structure, either 1,3 or 1,1 position of urea, supports the DMU as a model compound of urea with lower reactivity compared to urea. The reaction of DMU with formaldehyde limits certain intermediate products and side reactions, thereby making the reaction easier to understand and analyze spectroscopically. DMU-formaldehyde resin does not crosslink as UF does, thus it can be analyzed more easily by NMR [72].

1.7 Aim and Scope of the Study

In this study, only the properties of the UF resin are considered as variables under investigation, while other factors, such as the characteristics of the wood particles and the processing conditions for wood composites, are maintained as controlled variables. This study primarily focused on understanding the formation of the methylene bridge and ether bridge in the UF reaction system, as well as the impact of increasing the methylene bridge content in the UF resin on wood composites. To increase the methylene bridge to ether bridge ratio, two approaches were taken: 1. changing the reaction parameters, and 2. incorporating the alkyl-substituted urea in the UF reaction. In this study, UF reaction pH, time, temperature, and the order of urea and formaldehyde addition were considered. One standard reaction that is well established in the literature and industrial practice was considered a standard reaction (Method-1), and all reaction parameters of the standard reaction remained as controlled variables. Through changing the reaction pH, time, temperature, and the order of urea and formaldehyde addition of the standard reaction, seven different methods of UF resin synthesis were established. The primary aim for synthesizing UF under different conditions was to improve the methylene bridge contribution in the UF crosslinking structure. The second approach of this study is to incorporate 1,3 DMU and 1,1 DMU at different percentages in the UF reaction system. The target of incorporating the alkyl-substituted urea in the UF resin was to understand how it affects the methylene to ether bridge ratio, physical properties of the resin, the mechanical properties of the wood composites, and formaldehyde emission.

1.8 Challenges and Research Gaps

Although a number of approaches have been taken to improve the UF resin in terms of increasing the hydrophobicity and reducing the formaldehyde emission, incorporating 1,1 and 1,3 DMU into the UF resin to understand the impact on the physical properties of the resin, formaldehyde emission, and the mechanical properties of wood composites is very limited. Steinhof et al. investigated the 1,3 DMU-formaldehyde (DMUF) reaction and concluded as a model system of the UF reaction [72]. However, this study is very limited in understanding the reaction mechanism through the NMR technique and has no discussion on the wood composites side. Furthermore, there is a very limited study on 1,1 DMUF and its impact on resin properties and curing behavior. Despite having a general overview of methylene and ether bridge formation conditions, there are very limited studies that directly discuss the effects of changing the reaction pH, time, temperature, and order of urea formaldehyde addition on the ratio of methylene to ether bridge, and ultimately, its impact on wood composites is very limited. Many articles report the impact of the F/U ratio on formaldehyde emissions and discuss the impact of crystallinity [8]. However, there is very limited research on changing the order of urea and formaldehyde addition to change the properties of UF resin and how it impacts the formaldehyde emission and properties of wood composites.

1.9 Justification and Novelty of this Study

To address the mentioned knowledge gap, this study focuses on two approaches with the ultimate goal of improving and investigating the UF resin. Unlike previous studies, our work focuses on improving the hydrophobicity of the UF resin through increasing the ratio of methylene to ether bridge compared to the standard UF resin (Method-1). To increase the methylene bridge content, seven more reactions are completed by changing pH, time, temperature, and order of adding urea and formaldehyde. Although there is a general understanding of methylene and ether bridge formation conditions, UF reactions (methods 2 to 6) specifically give a correlation between the reaction parameters and the methylene and ether bridge content. Our findings offer a new direction for understanding the properties of wood composites, fabricated using all eight resins. Moreover, the impact on the properties of wood composites by changing resin properties is also investigated here. On top of that, this study gives a direct correlation between changing the reaction parameters and their impact on the formaldehyde emission.

Although numerous studies have been conducted on incorporating different types of modifiers and fillers to improve the resin properties, the question of incorporating 1,3 DMU and 1,1 DMU in the UF system remains unanswered. There is a lack of research on 1,1 DMU as a model system for UF resin, and the reaction limitations of using 1,1 DMU remain unclear. A unique feature of this study is that 1,3 DMU and 1,1 DMU were incorporated to understand the impact on reaction mechanisms, curing behavior, and formation of methylene bridge and ether bridge. To the best of our knowledge, this is the first study to investigate the incorporation of alkyl-substituted urea and its impact on the formaldehyde emissions and wood composite properties. This study presents a new perspective on using the urea model compound in UF resin and describes the limitations.

1.10 Characterization Techniques Used in this Study

After synthesizing the resin, all physical parameter tests, including gel time, viscosity, solid content percentage, density, and pH of the resin, were completed and recorded for all resins synthesized in this study. These provide fundamental information about the resin and help us compare them to other formulations. To understand the formation of the methylene and ether bridges, the NMR spectroscopy technique was used. The integrated areas that correspond to the methylene protons of the methylene and ether bridges were considered. The final calculation considered two protons for the methylene bridge and four protons for the ether bridge. The raw integrated area was divided by two for the methylene bridge and by four for the ethylene bridge to find the final contribution from each proton. Additionally, FTIR spectroscopy was used to understand the structure of the UF resin. However, due to the presence of a number of -OH groups and water in the UF resin, it becomes very difficult to comprehend the analysis and differentiate between different resin formulations. TGA was used to understand the thermal behavior of UF resin and to find any change in the thermal profile due to the change in the resin synthesis procedures or incorporation of alkyl-substituted urea model compounds. To understand the curing behavior of the synthesized resin, dynamic DSC and temperature sweep Rheology study were conducted. Finally, the board performance tests, including mechanical properties of boards, water absorption and retention, and formaldehyde emission were conducted to understand the impact of resin on the final properties of wood composites.

2 Impact of the Methylene-to-Methylene Ether Bridge Ratio on the Structural Characteristics and Performance of Urea-Formaldehyde Resins in Wood Composites

2.1 Design and Synthesis of UF Resins

2.1.1 Materials

Formaldehyde solution (37% w/v) was obtained from Kastamonu Entegre. Urea (ultra-pure grade, ≥99%) was purchased from Bio Basic, while ammonium chloride (≥99.9%) was purchased from Merck. Formic acid (85% w/v) and sodium hydroxide solution (24% w/v) were purchased from Albar Kimya and used after appropriate dilution to the desired concentrations. Melamine (99%) was supplied by Kastamonu Entegre. The Wood particles were received from Kastamonu Entegre with a specific moisture content.

2.1.2 Synthesis of UF Resins

2.1.2.1 Synthesis of Standard/Reference UF Resin (Method-1)

Step-1: Methylolation (**Figure 9**)

The synthesis was initiated in a four-neck round-bottom flask equipped with a mechanical stirrer, a reflux condenser (central neck), and a thermocouple (second neck). Into the flask, 37% (w/v) formaldehyde solution was introduced. Continuous stirring at 250 rpm was maintained throughout the reaction. The pH of the solution was adjusted to 8.5 by the gradual addition of a 10% (w/v) sodium hydroxide (NaOH) solution, with real-time monitoring using a calibrated digital pH meter. Once the desired pH was achieved, the first urea (formaldehyde to urea mole ratio is 2.1) was added via the third neck. The reaction mixture was initially heated to 45°C, followed by a controlled temperature increase to 80°C for 10 min to promote methylolation.

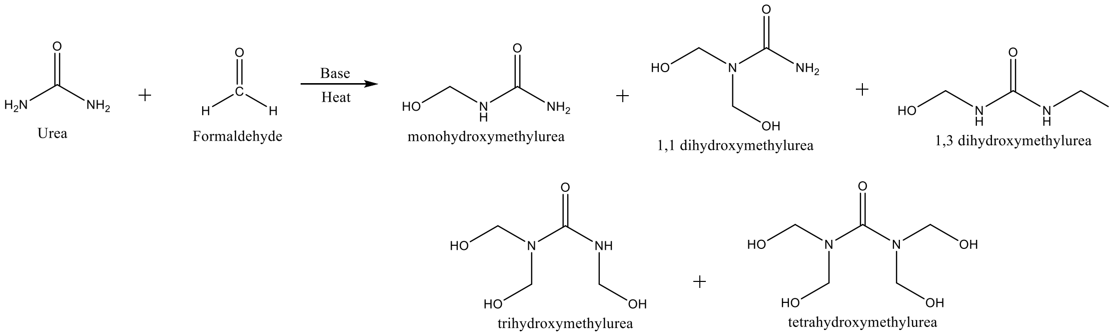

Figure 9. Methylolation or addition reaction of UF resin

Step-2: Condensation (**Figure 10**)

Following the methylolation stage, the pH of the reaction mixture was carefully lowered to 5.0 using a 40% (w/v) formic acid solution and monitored continuously via the pH meter. Simultaneously, the reaction temperature was increased from 80°C to 98°C. This condensation phase was maintained for approximately 2.5 h, with the progression of the reaction monitored by measuring the viscosity at regular intervals. The reaction was considered complete once the viscosity reached the target range of 33-40 centipoise (cP). At this point, the pH was readjusted to 8.5 with 10% (w/v) NaOH.

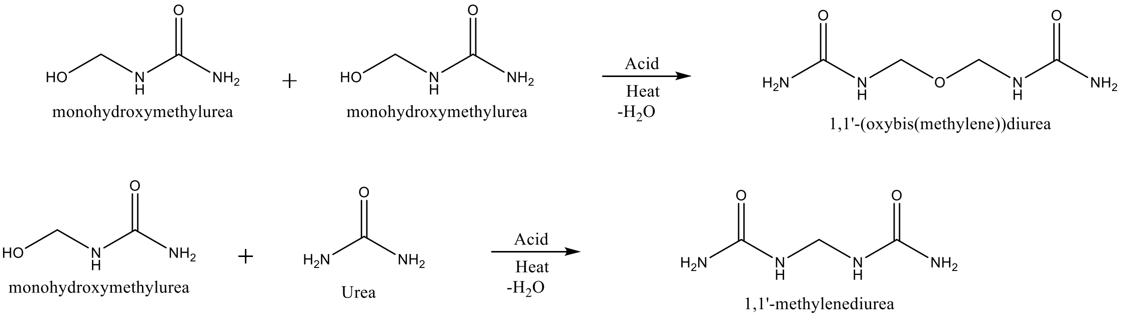

Figure 10. Condensation reaction of UF resin

Step-3: Post-condensation and final urea addition

Upon completion of the condensation reaction, the mixture was allowed to cool to 45°C, and a second urea was added to the flask (formaldehyde to urea mole ratio is now 1.1). Stirring was continued at 250 rpm for 1 h. The resulting UF resin was then transferred into a sealed one-neck flask and stored at room temperature.

2.1.2.2 Potential Yet Unlikely Side Reactions: A Theoretical Consideration

There are possible side reactions during the UF synthesis, which are shown in **Figure 11**.

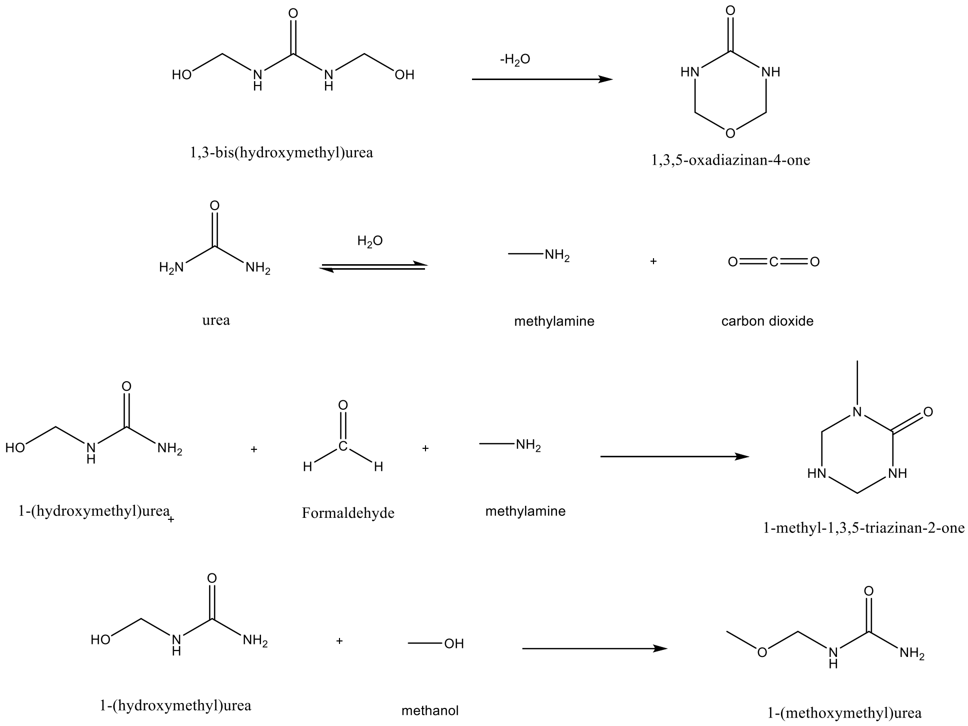

Figure 11. Side reactions of the UF system

2.1.2.3 Synthesis of UF Resin with Seven Different Methods (Deviation from Standard)

1.1.1.1.1 Method-2

Instead of 80 °C at pH 5.5, the reaction was carried out at 98 °C with the pH adjusted to 5.0. After 2 h of reaction, the second portion of urea was added.

1.1.1.1.2 Method-3

The first urea was added gradually within 30 minutes rather than adding it once. During the urea addition, the temperature gradually increased and was adjusted to 98 °C, with the pH set to 5.0 instead of the initial 80 °C and pH 5.5.

1.1.1.1.3 Method-4

Water was added together with the first portion of urea at the beginning of the process, and a urea-water solution was prepared. The pH was adjusted to approximately 8.5, and the temperature was increased to 80 °C before the formaldehyde was added dropwise. The addition of formaldehyde lasted approximately 1 h, during which the pH was maintained above 8.5. Subsequently, the temperature was increased to 98 °C, and the pH was adjusted to 5.0.

1.1.1.1.4 Method-5

Water was added together with the first portion of urea at the beginning of the process, and a urea-water solution was prepared. The pH was adjusted to approximately 8.5, and the temperature was increased to 98 °C before the formaldehyde was added dropwise. The addition of formaldehyde lasted approximately 1 h, during which the pH was maintained above 8.5. Subsequently, the temperature was kept at 98 °C, and the pH was adjusted to 5.0.

1.1.1.1.5 Method-6

Water was added together with the first portion of urea at the beginning of the process, and a urea-water solution was prepared. The pH was adjusted to approximately 8.5, and the temperature was increased to 98 °C before the formaldehyde was added dropwise. The addition of formaldehyde lasted approximately 2 h, during which the pH was maintained above 8.5. Subsequently, the temperature was kept at 98 °C, and the pH was adjusted to 5.0.

1.1.1.1.6 Method-7

Water was added together with the first portion of urea at the beginning of the process, and a urea-water solution was prepared. The pH was adjusted to approximately 8.5, and the temperature was increased to 98 °C before the formaldehyde was added dropwise. The addition of formaldehyde lasted approximately 3 h, during which the pH was maintained above 8.5. Subsequently, the temperature was kept at 98 °C, and the pH was adjusted to 5.0.

1.1.1.1.7 Method-8

Water was added together with the first portion of urea at the beginning of the process, and a urea-water solution was prepared. The pH was adjusted to approximately 8.5, and the temperature was increased to 98 °C before the formaldehyde was added dropwise. The addition of formaldehyde lasted approximately 4 h, during which the pH was maintained above 8.5. Subsequently, the temperature was kept at 98 °C, and the pH was adjusted to 5.0.

2.1.3 Synthesis of Standard/Reference MUF

Step-1: Methylolation (**Figure 12**)

The reaction was carried out in a 1000 mL three-necked round-bottom flask. The middle neck of the flask was connected to a reflux condenser, while an external thermometer was placed in the second neck to precisely monitor the reaction temperature. The first step involved a 37% formaldehyde solution in the reactor. The magnetic stirrer set at 600 rpm ensured homogeneous mixing throughout the reaction. To regulate the pH of the reaction, the target pH was adjusted to 5.0 using a 10% sodium hydroxide (NaOH) solution. Precise pH monitoring was achieved using a digital pH meter. Then, melamine and then the first urea were added through the third neck of the flask. In this formulation, the molar ratio of formaldehyde to melamine is 5.7, the formaldehyde to urea molar ratio is 3.4, and the overall formaldehyde to urea–melamine molar ratio is 2.1. The reaction temperature was initially 45°C, gradually increased to 70°C, and kept at this temperature for 10 min.

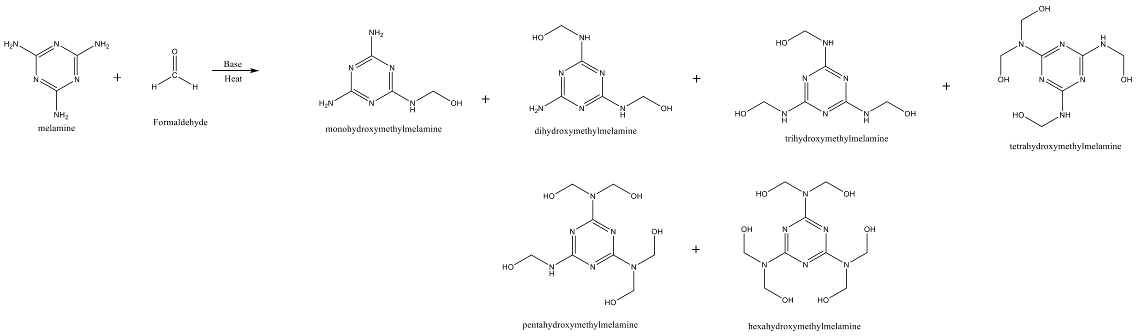

Figure 12. Methylolation or addition reaction of MUF resin

Stage-2: Condensation (**Figure 13**)

After 10 min, the reaction was monitored at 70°C, and the pH was set between 7.00-7.20 with NaOH solution. The progress of the reaction was followed by flow time (Fordcup method). When the flow time (at the reaction temperature) reached 20-23 seconds, the pH of the reaction was increased to 8.8 by the addition of NaOH solution, and the reaction was stopped (approximately 1 h).

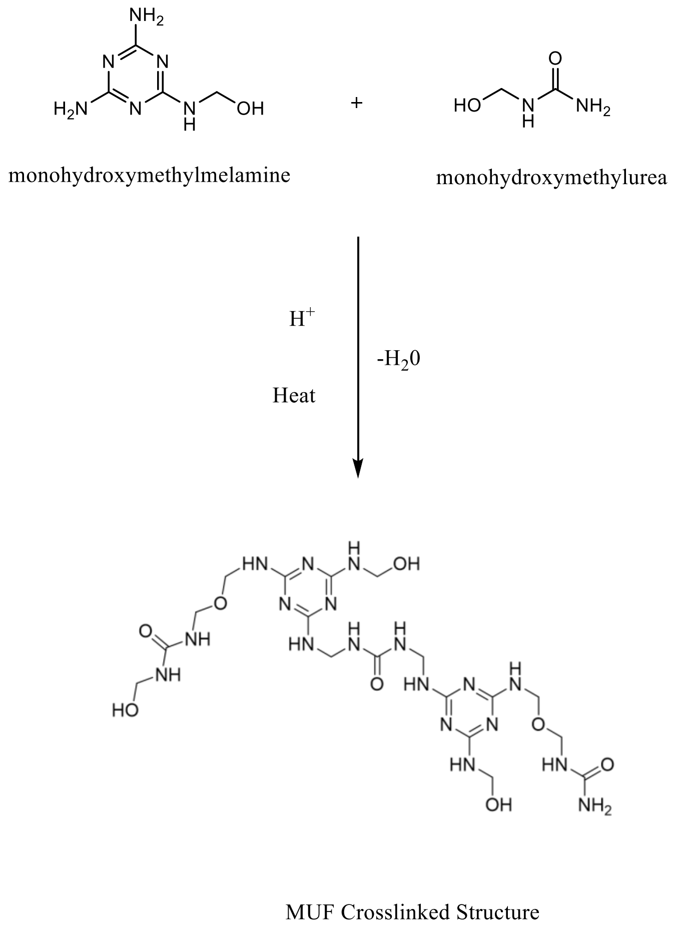

Figure 13. Condensation reaction of MUF resin

Step-3: Post-condensation and final addition of urea

The reaction mixture was then rapidly cooled to 45°C. In the cooling step, a second urea (formaldehyde to urea–melamine molar ratio is 1.1) was added to the reactor at a temperature of 45°C. The reaction was stirred with a magnetic stirrer for 1 h. After the reaction was completed, the resin was placed in a sample container and stored at room temperature.

2.1.4 Preparation of Wood Composites

Three-layer laboratory-scale particleboards, each measuring 400 mm × 400 mm × 16 mm, were fabricated, comprising two surface layers and a central core layer. UF resin served as the adhesive, applied at a rate of 7 wt% for the surface layers and 11.5 wt% for the core layer, relative to the oven-dry weight of the wood particles. Before adhesive application, the wood particles were conditioned to a moisture content of approximately 4%. The mat structures were then manually formed and subjected to hot pressing at 200°C under a pressure of 100 bar for 5 min. The particleboards were produced with a target density of 640 kg/m^3.

2.1.5 Instruments

FTIR spectra were obtained using a ThermoScientific Nicolet iS50 FTIR spectrometer. ^{1}H-NMR analysis was carried out with a 60 MHz Benchtop spectrometer with DMSO-d_6 solvent. Thermogravimetric analysis (TGA) was conducted with the Mettler Toledo TGA 2 Star System instrument at a range of 25°C to 800ºC with a 10°C/min heating rate and 20 ml/min nitrogen flow. Differential scanning calorimetry (DSC) analysis was performed with the Mettler Toledo DSC 3 Star System instrument with sample sizes of 8-10 mg. DSC thermograms were obtained with dynamic mode from 25°C to 300°C at a 10°C/min heating rate. All DSC studies were conducted under a nitrogen flow of 20 mL/min. The onset temperatures of thermal degradation were obtained where the tangent line at the inflection point of the DSC thermogram intersected with the baseline drawn at the point where the descent of the curve occurred. Viscosity measurements were conducted using a Brookfield DV2T viscometer with a SC4-2 1 type spindle. All samples were tested within the linear viscoelastic limit, and a 0.5 mm gap between the plates was maintained. The temperature sweep of the rheology test was conducted at temperatures from 25ºC to 200ºC with a linear 2ºC/min increment. To evaluate the gel time in the physical testing of the resin, 5 g of a 10% (w/w) aqueous ammonium chloride solution was added to 50 g of resin in a beaker. The mixture was stirred thoroughly until a homogeneous composition was obtained. A representative aliquot of the prepared mixture was then transferred into a test tube, into which a metal rod was placed. The test tube was subsequently immersed in a boiling water bath maintained at 100 °C. At this point, a stopwatch was initiated. Stirring was continued manually with the metal rod, and the stopwatch was stopped at the onset of resin solidification. The elapsed time, recorded in seconds, was designated as the gel time. All pH measurements were performed using a Mettler Toledo pH meter. Before measurement, the electrode was immersed in the sample cooled to 20°C, and the pH value was recorded once it stabilized. The viscosity of the resin was measured using a Brookfield cap-cone type viscometer at 20°C. To measure the density of the resin, the resin was cooled to 20°C and kept in a 250 mL beaker. An appropriate hydrometer was carefully immersed in the sample, and the system was allowed to stabilize. Once the hydrometer reached equilibrium, the value indicated on the scale was recorded as the density of the resin, expressed in g/cm^3. To determine the solid content, a minimum of 1 g of resin sample was weighed into pre-weighed (tared) aluminum containers. For each sample, three replicates were prepared. The samples were then placed in a drying oven at 120 °C for 2 h. After the heating period, the containers were cooled to room temperature and reweighed. The solid content (%) was calculated using the following equation: Solid content% = (Weight after drying − Tare) × 100 / (Initial Weight − Tare). **Table 3** outlines the performance evaluation methods employed for wood composites.

2.2 Characterization of Standard/ Reference UF and MUF Resin

2.2.1 Structural Analysis of Standard/ Reference UF and MUF Resin

2.2.1.1 FTIR

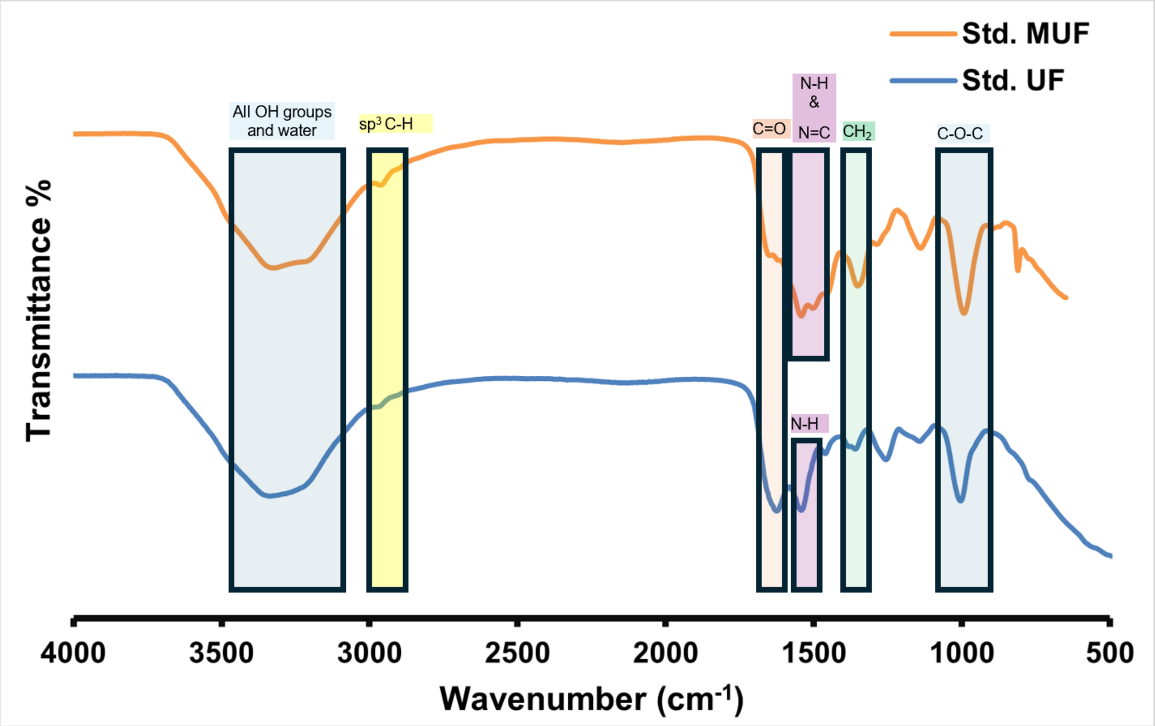

Figure 14. FTIR of reference UF and MUF

For both UF and MUF resins, the presence of hydroxyl groups (-OH) and water is observed as a broad absorption band in the range of 2900 cm^{-1} to 3650 cm^{-1} due to the strong hydrogen bonding effect. The stretching vibration observed at 2955 cm^{-1} in MUF and 2960 cm^{-1} in UF is attributed to sp^3-hybridized C–H stretching, which originates from sp^3-hybridized carbon and is partially obscured by the OH stretching. The strong peaks appearing at 981 cm^{-1} in MUF and 1003 cm^{-1} in UF are due to C–O–C stretching vibrations. For UF, the corresponding peak is relatively weaker compared to MUF. Both MUF and UF exhibit weak signals at 1347 cm^{-1} and 1358 cm^{-1} corresponding to CH_2 bending vibrations. In UF, a strong carbonyl (C=O) stretching band is observed due to changes in dipole moment, typically appearing at 1620 cm^{-1}. In contrast, this region in MUF is highly complex due to the presence of conjugated C=N bonds with delocalized

π-electron clouds and carbonyl (C=O) stretching, resulting in a significantly split absorption pattern. In UF, the N-H peak is observed at 1543 cm^{-1}. The N-H vibration overlapped with the N=C vibration in MUF is observed at 1499 to 1542 cm^{-1}.

2.2.1.2 NMR

To gain deeper insight into the structural characteristics of UF resins, ^1H NMR spectroscopy was employed. As illustrated in **Figure 15**, chemical shifts corresponding to all protons associated with UF resin structures were detected, alongside identifiable peaks for DMSO-d_6, water, and HOD. DMSO-d_6, used both as solvent and external reference, exhibited a characteristic singlet at 2.5 ppm. The HOD and water signals appeared within the range of 3.7–4.1 ppm for samples synthesized via Method-1 through Method-4. Notably, methanediol (formaldehyde monohydrate or methylene glycol or oxymethylene glycol) resonates within the same region, resulting in a broad, composite peak with minor shoulder signals.

From Method-5 onwards, this peak region experienced a shift to 3.0–3.5 ppm, suggesting a shielding effect. This shift can be attributed to structural changes in the UF resin arising from modifications in the order of urea and formaldehyde addition during the reaction. The NMR samples analyzed represent the final resin products, where the hydroxyl functionalities are expected to be substantially consumed. In Method-1 through Method-4, methoxymethanol (hemiformal) signals are evident, but they disappear in Methods 5–7. This trend is directly correlated with the synthesis protocol: in Methods 1–3, urea was added to the formaldehyde solution, whereas in Methods 4–7, formaldehyde was introduced into an aqueous urea solution. However, Method-4 differs due to the relatively lower methylolation temperature (80 °C), which likely inhibited methylene bridge formation and subsequently resulted in a spectral profile resembling that of Method-1.

Hemiformal formation occurs only under conditions of excess formaldehyde, which is satisfied in Methods 1–3. In contrast, the energy barrier at 80 °C in Method-4 restricts further condensation, preventing effective crosslinking. The characteristic resonance for amine protons (N–H) is typically observed between 8.5–9.0 ppm. However, such signals were not detected in any of the UF resin samples, likely due to limitations of the NMR instrument and hydrogen bonding effects, which can obscure N–H visibility in low-field spectra. High-field NMR instrumentation would be required for the reliable detection of these protons.

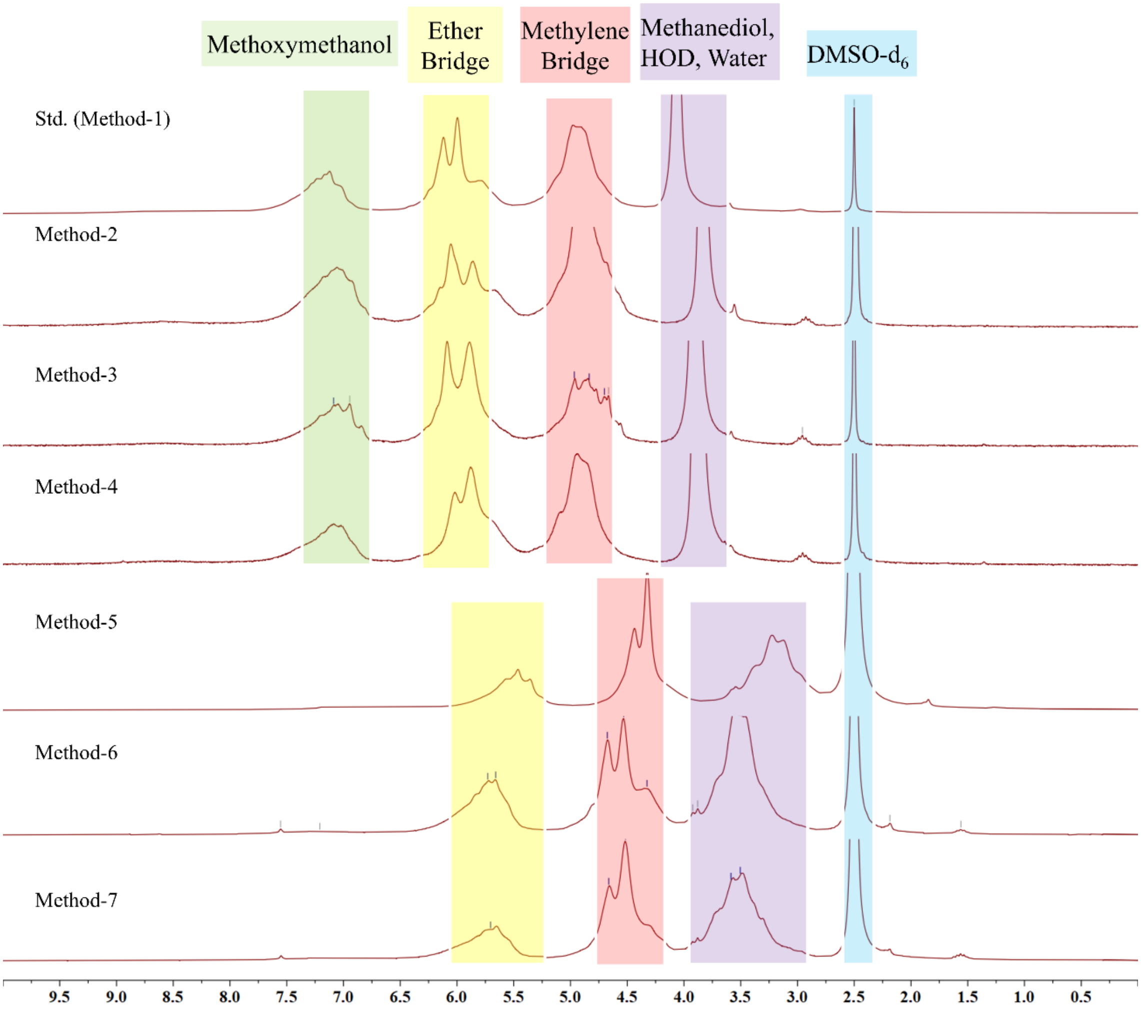

Figure 15. ^{1}H NMR data of all UF resins

The primary objective of this NMR investigation was to identify and quantify the methylene and ether bridges, the two most critical crosslinking motifs in the UF network. The methylene bridge appeared within 4.5–5.5 ppm for Methods 1–4 and shifted slightly to 4.0–5.0 ppm for Methods 5–7. Similarly, ether bridges resonated at 5.5–6.5 ppm in Methods 1–4, shifting to 5.0–6.0 ppm in Methods 5–7. The relative intensities of these peaks, derived via peak integration, offer a quantitative means to estimate the bridge ratio. Importantly, the methylene bridge is generally associated with increased hydrophobicity, whereas the ether bridge contributes to hydrophilicity. Therefore, this ^{1}H NMR analysis provides critical structural insights into the hydrophilic–hydrophobic balance of UF resins synthesized under varying reaction conditions, offering a valuable foundation for tailoring resin properties through synthetic control.

2.2.2 Thermal Stability and Curing of Standard UF Resin

2.2.2.1 TGA

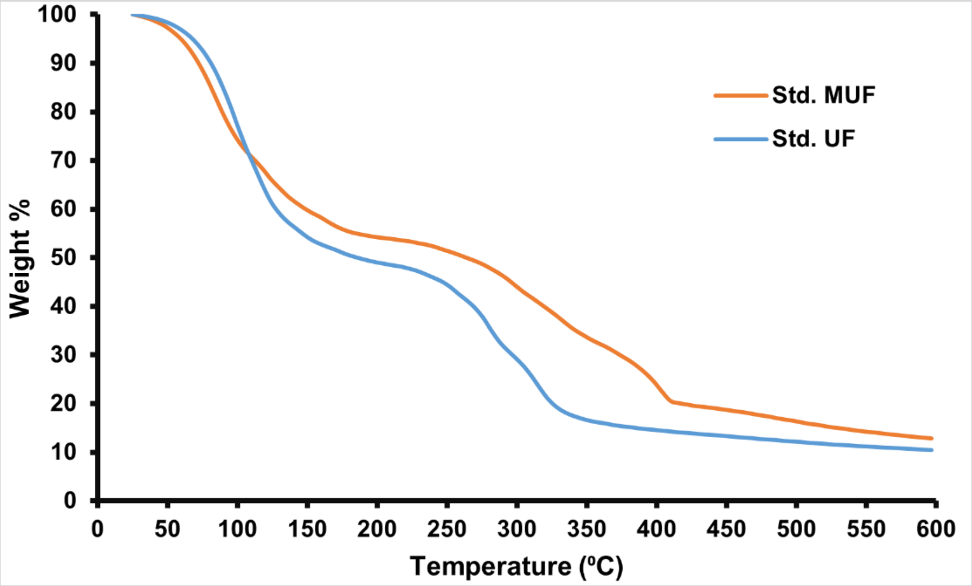

Figure 16. TGA thermograms of reference UF and MUF resins

Thermogravimetric analysis (TGA) was conducted to assess the thermal stability and decomposition behavior of UF and MUF resins, with the results presented in **Figure 16**. The TGA profiles reveal that both resins exhibit a two-step degradation process: an initial mass loss attributed to the evaporation of water, followed by thermal decomposition of the polymer network. Approximately 50% weight loss was observed around 100°C for both UF and MUF, indicating a high water content, consistent with the resins retaining roughly 50% water by weight due to the condensation reaction releasing water, and 37% formaldehyde solution is used in the reaction.

As the temperature increased, substantial degradation of the resin matrix was evident. By 350°C, the UF resin had lost nearly 80% of its initial mass, whereas the MUF resin showed a comparatively lower mass loss of approximately 70%. At 600°C, the cumulative mass loss reached approximately 80–90% for both systems. However, MUF demonstrated improved thermal stability relative to UF, which can be primarily attributed to the incorporation of melamine, a compound with a thermally stable triazine ring. The enhanced thermal resistance of MUF is further supported by its heterocyclic structure and the more complex, highly branched network that results in a higher crosslinking density compared to UF.

Additionally, the char residue at 600 °C was greater for MUF than for UF, reflecting the inherent structural stability and carbon-rich composition of the melamine component.

This higher residual char content is indicative of greater thermal resistance and supports the inference that MUF-based wood composites are likely to exhibit superior performance under elevated temperatures when compared to their UF-based counterparts.

2.2.2.2 Dynamic DSC

To investigate the curing behavior of MUF and UF resins, dynamic DSC analysis was performed, as shown in **Figure 17**. Characterizing the curing behavior of UF and MUF resins via DSC presents significant challenges, primarily due to the high water content inherent in these systems. The presence of water leads to fluctuations in the DSC thermal baseline, making it difficult to identify clear and reproducible curing peak temperatures. Although some studies attempt to eliminate water prior to DSC analysis to improve signal clarity, such approaches fail to accurately represent the in-situ curing behavior encountered in industrial applications, thereby resulting in curing profiles that lack practical relevance. An alternative and more representative method involves conducting DSC measurements using a pressurized pan system to minimize the interference from water evaporation. During heating, water evaporation near 100 °C produces a pronounced endothermic peak, which overlaps and partially masks the exothermic heat released during resin curing. Furthermore, the methylolation reaction is an endothermic process, which also contributes to the distortion of the exothermic curing peak. In addition, as the condensation reactions proceed over a wide temperature range from the onset of curing, the resulting water is continuously released and subsequently evaporated, producing additional endothermic effects. From the thermograms, it is evident that MUF resin initiates curing at a lower temperature than UF resin, despite exhibiting a relatively lower exothermic peak and being less easily identifiable. This earlier onset, beginning around 80 °C for MUF compared to approximately 100 °C for UF, is attributed to the higher intrinsic reactivity of melamine (6 reactive sides) over urea (4 reactive sides). A broad endothermic peak observed near 110 °C in the MUF sample likely corresponds to water release and evaporation associated with condensation reactions. In contrast, a pronounced endothermic peak around 200 °C in the UF sample may be indicative of resin degradation.

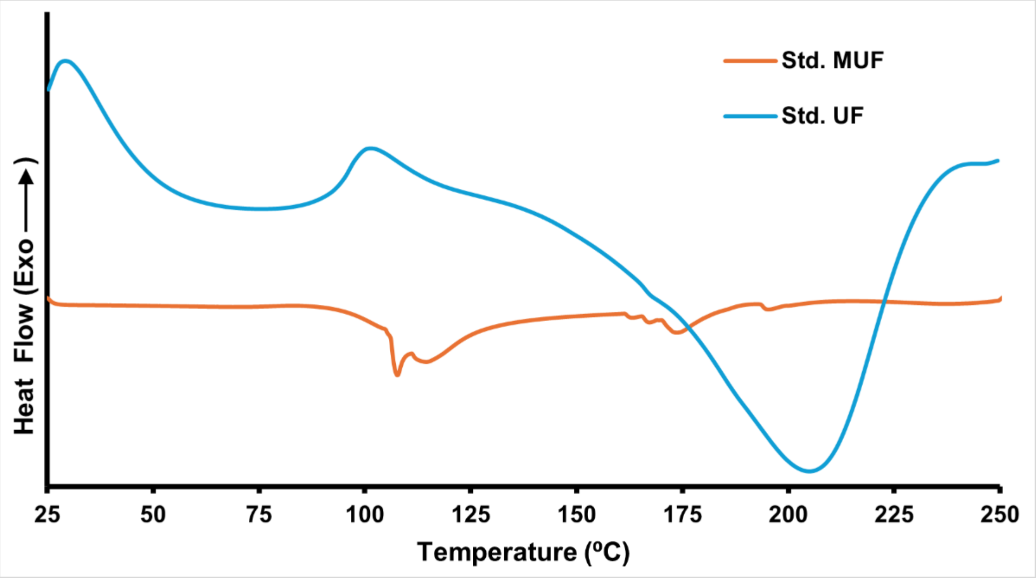

Figure 17. Dynamic DSC thermograms of reference UF and MUF

It is critical to recognize that during the curing process of both UF and MUF resins, exothermic and endothermic processes occur concurrently. The dominant thermal event observed in the DSC thermogram is often the result of competing effects, where exothermic curing reactions are partially or fully offset by overlapping endothermic phenomena, such as water evaporation and methylolation.

2.2.3 Rheology Study

To investigate the viscoelastic behavior of UF and MUF resin, a temperature sweep rheology test was conducted and presented in **Figure 18**. From the complex viscosity analysis of the UF and MUF resin, it is very clear that MUF starts curing earlier than UF. The onset of cure is around 105°C for MUF and 125°C for UF. The expected cure of MUF starts earlier compared to the UF system due to its more reactive and higher number of amine groups. The rheology results also confirm the dynamic DSC tests, where MUF also started curing earlier than UF.

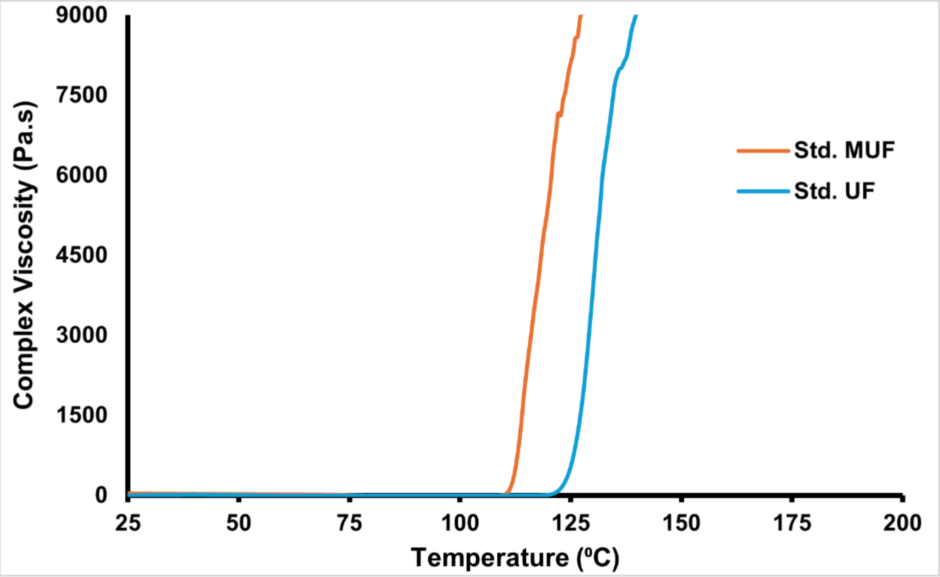

Figure 18. Rheology of reference UF and MUF

2.3 Characterization of UF Resin (Method 2 to Method 8)

2.3.1 Physical Properties of Resins

The physical properties of UF resins, including pH, viscosity, gel time, density, and solid content, were evaluated 24 h after the completion of resin synthesis. The results for all formulations (Method-1 (Std. UF) to Method-8 and reference MUF) are summarized in **Table 1**. These parameters are critical for understanding resin formation mechanisms, processability, and performance in wood composite manufacturing. Moreover, they offer valuable insights into curing behavior, optimal hardener requirements, curing time, and the expected density, thickness, and overall quality of the resulting wood-based composites.

Table 1. Physical properties of all resins

Physical Properties of Synthesized Resins									
	Std. UF	Std. MUF	Method-2	Method-3	Method-4	Method-5	Method-6	Method-7	Method-8
pH	8.3	9.13	9.1	7.75	8.04	8.1	8.3	7.75	8.04
Viscosity mPa.s (20^{o}C)	21	161	31	35.3	33.8	36	34	35.3	33.8
Gel time (s)	47	51	51	80	75	76	78	80	116
Density (g/cc)	1.214	1.24	1.203	1.215	1.21	1.213	1.214	1.215	1.21
Solid content (%)	54	56.37	49.32	52.67	53.53	52.13	52.25	52.67	53.35

The final pH of resins was adjusted to 8.5 for UF and 8.8 for MUF, without the use of buffering agents. However, pH measurements taken after 24 h indicated slight deviations, attributable to the continued condensation reactions occurring at ambient temperature. In some cases, such as MUF and Method-2, a slight increase in pH was observed, which could result from ongoing methylolation reactions or urea decomposition under alkaline conditions, though such increases are relatively uncommon. Conversely, most methods showed a minor decrease in pH, likely due to hydrolysis of intermediate species, degradation of methylene bridges, or oxidation of residual formaldehyde. These small changes indicate reasonable room temperature stability of the synthesized resins.

MUF resin exhibited slightly higher viscosity compared to all UF resin formulations. Viscosity in amino resins is generally correlated with crosslinking density; thus, the higher viscosity of MUF can be attributed to the increased functionality of melamine (six reactive sites) relative to urea (four reactive sites), leading to a more extensively branched network. The viscosity values of the UF samples synthesized via Methods 1–8 remained relatively consistent with one another.

The gel time of amino resin is defined by the time required to convert the liquid resin into a solid material at a specific temperature and conditions. This is one of the fundamental parameters that determine the quality of resin, curing behavior, and processing conditions. All UF resin formulations displayed higher gel times than the standard UF resin benchmark (47 s), suggesting limited crosslinking capability and slower network formation. Increased gel time is typically associated with challenges in curing efficiency and may result in inferior mechanical performance of the final wood composite. Although extended gel time may enhance storage stability, it often correlates with higher formaldehyde emissions, prolonged curing cycles, and reduced productivity. Among the formulations, Method-8 exhibited the highest gel time (116 s), followed by Method-7 and Method-3 (80 s), Method-6 (78 s), Method-5 (76 s), and Method-4 (75 s), with Method-2 (51 s) being closest to the standard UF value. The reference MUF resin displayed a gel time of 51 s, comparable to the standard UF.

As the F/U molar ratio and formaldehyde concentration (37%) were kept constant across all syntheses, minimal variation was observed in the density of the UF resins. MUF, owing to the incorporation of melamine, exhibited a slightly higher density (1.40 g/cm^3) compared to UF (1.20 g/cm^3). All UF resins maintained a density close to 1.20 g/cm^3. A similar trend was observed in solid content measurements, with MUF exhibiting a higher solid content (56.37%) compared to UF (54.0%). Minor variations in solid content among the UF formulations were observed—Method-2 having the lowest and Method-8 the highest, primarily due to differences in the extent of condensation and water release during synthesis.

Interestingly, despite having the highest solid content, Method-8 also exhibited the longest gel time. This apparent discrepancy may be explained by variations in the formation ratios of methylene and ether bridges, which play a critical role in the crosslinking density and thermal reactivity of the resin network.

2.3.2 Understanding the Methylene and Ether Bridge Formation

To evaluate the hydrophobic and hydrophilic characteristics of the synthesized urea-formaldehyde (UF) resin, the relative proportions of methylene and ether bridges were quantified using ^{1}H NMR spectroscopy. The analysis considered the proton signals corresponding to methylene ($-CH_2-$) and ether ($–CH_2–O–CH_2–$) linkages. The raw integrated peak areas were obtained and subsequently normalized by dividing the area by 2 for methylene bridges and by 4 for ether bridges, corresponding to the number of protons contributing to each signal. The relative contributions of methylene and ether bridges within the polymer network were then estimated under the assumption that only these two types of linkages are formed during crosslinking, excluding the possibility of the formation of cyclic structures. The percentage contributions of methylene and ether bridges are summarized in **Table 2**.

Table 2. Methylene and ether bridge calculation for all UF resins

	Raw Integrated Area (Not Normalized)		Area Corresponding to Each proton		Ratio	Contribution to Structure (%)		Change in Methylene Bridge% (Compared to the Standard UF)
	Methylene Bridge	Ether Bridge	Methylene Bridge	Ether Bridge	Methylene to Ether Bridge	Methylene Bridge	Ether Bridge	
Standard UF	2.25	2.82	1.125	0.705	1.60	61.48	38.52	N/A
Method-2	2.19	1.78	1.095	0.445	2.46	71.10	28.90	15.65
Method-3	2.39	2.91	1.195	0.7275	1.64	62.16	37.84	1.10
Method-4	1.99	2.05	0.995	0.5125	1.94	66.00	34.00	7.36
Method-5	2.56	1.46	1.28	0.365	3.51	77.81	22.19	26.56
Method-6	3.76	2.08	1.88	0.52	3.62	78.33	21.67	27.41
Method-7	3.7	2.01	1.85	0.5025	3.68	78.64	21.36	27.91

A general trend was observed from the data, indicating that increasing the methylolation temperature from 80°C to 98°C and reducing the pH from 5.5 to 5.0 led to a higher methylene bridge formation. This trend is evident in Method 2, where the methylene bridge content increased by 15.65% compared to the reference method due to elevated temperature and lowered pH conditions. In contrast, the dropwise addition of urea appeared to have minimal influence on the formation of methylene bridges, as demonstrated in Method 3, which showed only a 1.1% increase compared to the reference.

Furthermore, altering the sequence of urea and formaldehyde addition can significantly affect methylene bridge formation, but only under specific reaction conditions. For instance, when methylolation was carried out at 98 °C and condensation at pH 5.0, a notable increase in methylene bridge content was observed. However, when the temperature remained at 80 °C and pH at 5.5, changing the order of addition resulted in only a slight increase of 7.36%.

Notably, in Method 5, where formaldehyde was added to a urea-water solution, reversing the order of the reference method, there was a substantial increase in methylene bridge content by 26.56%. The timing of formaldehyde addition, however, had a relatively minor effect. For example, in Methods 6 and 7, where formaldehyde was added over 2 h and 3 h, respectively, the methylene bridge content increased by 27.41% and 27.91%, values that are comparable to those observed in Method 5.

These results offer valuable insights into the underlying reaction mechanisms, the progression of the reaction, and the influence of specific conditions on the resulting product composition. The reversibility of the addition sequence of urea and formaldehyde significantly enhances the formation of methylene bridges. This is primarily due to the excess availability of urea in the reversed method, where formaldehyde is added to a urea-water solution, as opposed to the reference method, in which urea is gradually introduced into a formaldehyde solution, resulting in a comparatively urea-deficient environment.

Methylene bridges are predominantly formed through the reaction between methylol groups and urea, involving the substitution of a hydrogen atom on the urea molecule. The reversed addition sequence promotes this reaction by ensuring a higher concentration of urea relative to the available methylol groups, which are limited due to the restricted amount of formaldehyde. However, this effect is strongly dependent on the reaction conditions; the reversal in order is ineffective at lower temperatures and higher pH levels, where the formation of methylene bridges is limited.

Moreover, prolonging the formaldehyde addition time appears to have minimal to no influence on methylene bridge formation. This is because the formation of methylol groups is a prerequisite for the subsequent development of the methylene bridge. Without an adequate supply of formaldehyde, the formation of these intermediates is constrained.

2.4 Performance Analysis of Wood Composites

To evaluate the performance of the fabricated wood composites, a series of standardized tests were conducted, including internal bond (IB) strength, thickness swelling, water absorption, modulus of elasticity (MOE), modulus of rupture (MOR), and free formaldehyde content. The test results for wood composites prepared using the reference UF resin, reference MUF resin, and resins synthesized via Methods 5, 7, and 8 are summarized in **Table 3**. The test standard is also provided in the same table.

Table 3. Board test results of different resins

Property	**Measurement Parameter**	**Test Standard**	Std. UF (Method-1)					Std. MUF					Method-5				
			S-1	S-2	S-3	Avg.	CV (%)	S-1	S-2	S-3	Avg.	CV (%)	S-1	S-2	S-3	Avg.	CV (%)
Internal Bond Strength (IB)	Internal Bond Strength Average (N/mm²)	TS EN 319	0.38	0.38	0.40	0.39	3.15	0.47	0.45	0.49	0.47	3.62	0.60	0.57	0.60	0.59	2.77
	Average Density (kg/m³)	TS EN 323	658	642	653	651	1	678	673	687	679	1	725	715	716	719	0.73
Thickness Swelling	2-Hour Thickness Swelling Average (%)	TS EN 317	8.69	7.46	7.96	8.03	7.69	9.89	9.71	9.34	9.65	2.93	5.09	7.81	5.82	6.24	22.58
Water Absorption	2-Hour Water Absorption Average (%)	TS EN 317	43.00	36.56	43.08	40.88	9.14	48.79	59.11	44.69	50.86	14.61	19.88	25.36	21.51	22.25	12.65
Modulus of Elasticity / Modulus of Rupture (MOE / MOR)	Modulus of Rupture (MOR) Average (N/mm²)	TS EN 310	2027	2130	1980	2046	4	2160	2190	2363	2238	5	2610	2737	2820	2722	4
	Modulus of Elasticity (MOE) Average (N/mm²)	EN 310	8.88	10.04	9.35	9.42	6.17	10.87	11.28	12.20	11.45	5.97	14.00	15.93	15.20	15.04	6.49
	Board Thickness (mm)	TE EN 324-1	18	18	18	18	0	18	18	18	18	0.00	15	15	15	15.25	0.60
Free Formaldehyde Content	Board Moisture Content (%)	TS EN 322	6.58	6.79	6.90	6.76	2.41	6.74	6.29	6.83	6.62	4.37	5.98	6.17	6.33	6.16	2.84
	Formaldehyde Content	TS EN ISO 12460-5	9.47	9.28	9.08	9.28	2.10	7.27	7.30	7.34	7.30	0.48	8.99	8.72	8.61	8.77	2.23

Property	**Measurement Parameter**	**Test Standard**	Std. UF (Method-1)					Method-7					Method-8				
			S-1	S-2	S-3	Avg.	CV (%)	S-1	S-2	S-3	Avg.	CV (%)	S-1	S-2	S-3	Avg.	CV (%)
Internal Bond Strength (IB)	Internal Bond Strength Average (N/mm²)	TS EN 319	0.38	0.38	0.40	0.39	3.15	0.28	0.30	0.27	0.28	6.50	0.18	0.18	0.20	0.18	7.21
	Average Density (kg/m³)	TS EN 323	658	642	653	651	1	714	715	723	717.65	0.70	704	705	705	704.75	0.09
Thickness Swelling	2-Hour Thickness Swelling Average (%)	TS EN 317	8.69	7.46	7.96	8.03	7.69	13.75	11.06	9.53	11.45	18.67	17.85	14.04	18.72	16.87	14.74
Water Absorption	2-Hour Water Absorption Average (%)	TS EN 317	43.00	36.56	43.08	40.88	9.14	36.31	30.31	30.18	32.27	10.86	39.88	27.30	50.61	39.27	29.71
Modulus of Elasticity / Modulus of Rupture (MOE / MOR)	Modulus of Rupture (MOR) Average (N/mm²)	TS EN 310	2027	2130	1980	2046	4	3157	2833	3387	3126	9	2507	2850	2823	2727	7
	Modulus of Elasticity (MOE) Average (N/mm²)	EN 310	8.88	10.04	9.35	9.42	6.17	12.73	12.83	14.77	13.44	8.53	9.07	12.67	13.10	11.61	19.05
	Board Thickness (mm)	TE EN 324-1	18	18	18	18	0	16	16	16	15.92	0.32	16	16	16	15.84	0.39
Free Formaldehyde Content	Board Moisture Content (%)	TS EN 322	6.58	6.79	6.90	6.76	2.41	4.58	4.84	4.73	4.72	2.73	4.92	4.96	4.98	4.95	0.63
	Formaldehyde Content	TS EN ISO 12460-5	9.47	9.28	9.08	9.28	2.10	2.54		2.60	2.57	1.69	3.03	3.43		3.23	8.76

Overall, the particleboard fabricated using MUF resin exhibited superior performance across most measured properties compared to those prepared with UF resins. Notably, Method 5 yielded the highest internal bond (IB) strength among all tested formulations, surpassing both the reference UF and MUF resins. In contrast, IB strength decreased significantly in boards produced using Methods 7 and 8. This decline is attributed to the excessive formation of methylene bridges, which increases the hydrophobicity of the resin. The resulting incompatibility between the highly hydrophobic resin and the relatively hydrophilic wood particles adversely affects adhesion within the composite.

The wood composites prepared using Methods 5, 7, and 8 exhibited slightly higher densities compared to those produced with the standard UF and MUF resins, although the differences were marginal. Such variations can be attributed to minor deviations in the resin-to-wood ratio during panel fabrication. Additionally, inconsistencies in the hot-pressing pressure system and variations in the degree of resin curing may also contribute to the observed differences in composite density.

In terms of thickness swelling, Method 5 exhibited the lowest value among all formulations, indicating enhanced dimensional stability. In contrast, Method 8 resulted in a substantial increase in thickness swelling (almost twice that of reference UF), which can be primarily attributed to the poor compatibility between the resin and wood particles. This incompatibility likely led to the formation of voids within the wood composite structure, thereby increasing swelling. The reference UF and MUF resins, along with Method 7, showed comparable thickness swelling values.

For water absorption, Method 5 demonstrated the lowest absorption, indicating superior water resistance. In contrast, the composite prepared with MUF resin exhibited the highest water absorption among all samples. Method 8 and the reference UF resin showed comparable levels of water absorption, while Method 7 exhibited intermediate performance between these formulations. These results further support the enhanced moisture resistance achieved through the optimized resin structure in Method 5.

In terms of mechanical performance, Method 7 exhibited the highest modulus of rupture (MOR), followed by Methods 8 and 5, with the reference MUF and UF resins showing comparatively lower values. A similar trend was observed for the modulus of elasticity (MOE), with Method 7 again showing the highest value, followed by Methods 5 and 8, and then the reference MUF and UF resins. The board thickness across all samples was maintained within the range of 15–18 mm, with minimal deviation, ensuring consistency in the testing conditions.

Most notably, formaldehyde emission, a critical parameter for wood composites, was significantly reduced in Methods 7 and 8. The reference UF resin exhibited a formaldehyde emission of 9.28, while the MUF resin showed 7.30. Method 5 produced a slightly lower emission at 8.77. In contrast, Method 7 and Method 8 demonstrated dramatic reductions, with emissions of 2.57 and 3.23, respectively that is approximately one-third of the emission from the reference UF resin.

This substantial reduction can be attributed to the increased formation of methylene bridges in these methods. Methylene bridges are chemically more stable than ether bridges and less prone to hydrolysis, thereby reducing the release of formaldehyde. Moreover, the lower moisture content observed in the boards prepared with Methods 7 and 8 further supports this conclusion, as the hydrophobic nature of methylene bridges likely contributed to decreased water uptake and minimized formaldehyde release.

In conclusion, these findings underscore the importance of achieving an optimal balance in the hydrophobic–hydrophilic characteristics of UF resins. A resin with moderate hydrophobicity not only ensures better compatibility with cellulose-based materials but also enhances moisture resistance and contributes to reduced formaldehyde emissions.

3 Investigating the Performance of Wood Composites by Incorporating Alkyl-Substituted Urea Compounds into Urea-Formaldehyde Resin

3.1 Design and Synthesis of UF Hybrid Resin

3.1.1 Materials

Formaldehyde solution (37% w/v) was obtained from Kastamonu Entegre. Urea (ultra-pure grade, ≥99%) was purchased from Bio Basic, while ammonium chloride (≥99.9%) was purchased from Merck. Formic acid (85% w/v) and sodium hydroxide solution (24% w/v) were purchased from Albar Kimya and used after appropriate dilution to the desired concentrations. 1,3-Dimethylurea (1,3-DMU, 98%) and 1,1-Dimethylurea (1,1-DMU, ≥98%) were acquired from Thermo Scientific and used without further purification. Wood particles were received from Kastamonu Entegre with a specific moisture content.

3.1.2 Synthesis of UF Hybrid Resin

To investigate the influence of DMU on resin properties and wood composites, modified urea-formaldehyde (UF) resins were synthesized following the same procedure as the standard UF resin (UF-1). In these formulations, either 1,1-dimethylurea (1,1-DMU) or 1,3-dimethylurea (1,3-DMU) was partially substituted for urea during the first urea addition step of the synthesis. Specifically, 5 mol% and 10 mol% of 1,1-DMU were incorporated in UF-2 and UF-3, respectively, while 5 mol% and 10 mol% of 1,3-DMU were introduced in UF-4 and UF-5, respectively. The molar substitution ratios were calculated on a mole-to-mole basis relative to urea.

3.1.2.1 Methylolation

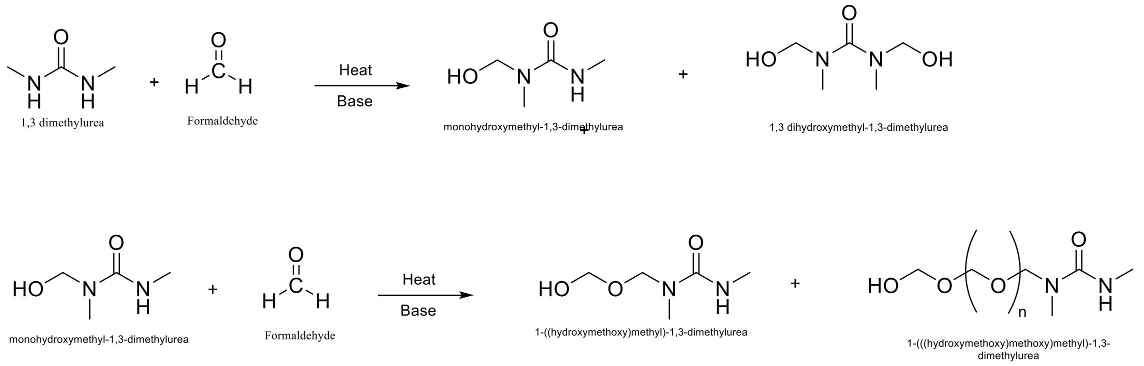

Figure 19. Methylolation of 1,3-DMUF

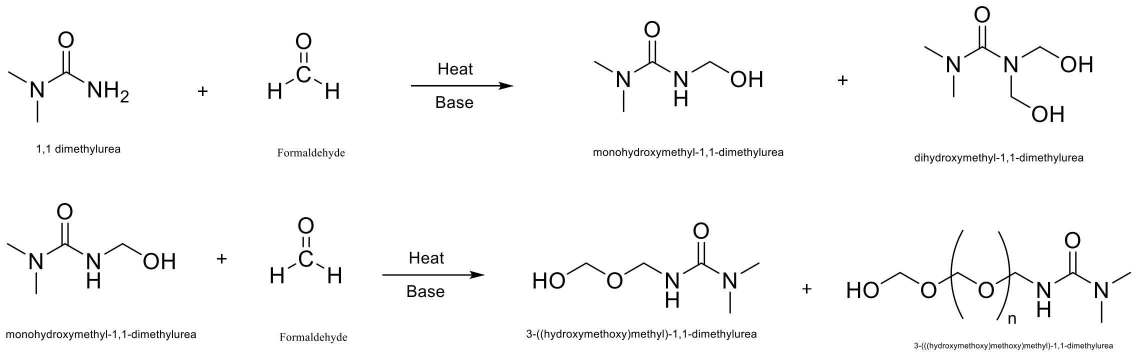

Figure 20. Methylolation of 1,1-DMUF

3.1.2.2 Condensation

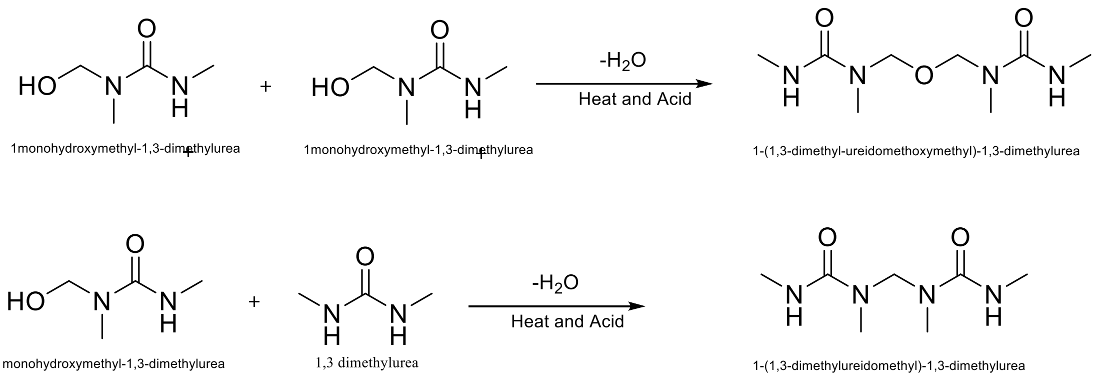

Figure 21. Condensation of 1,3-DMUF

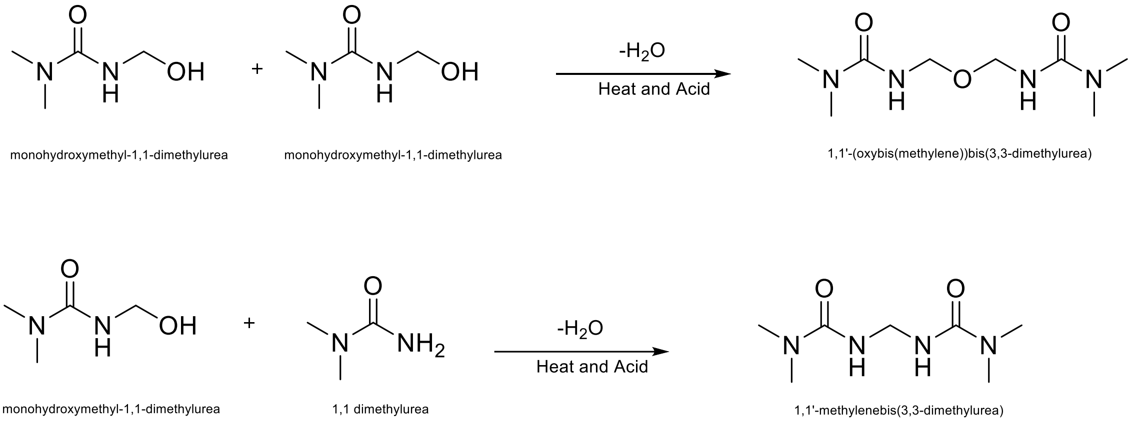

Figure 22. Condensation of 1,1-DMUF

3.1.3 Potential Yet Unlikely Side Reactions: A Theoretical Consideration

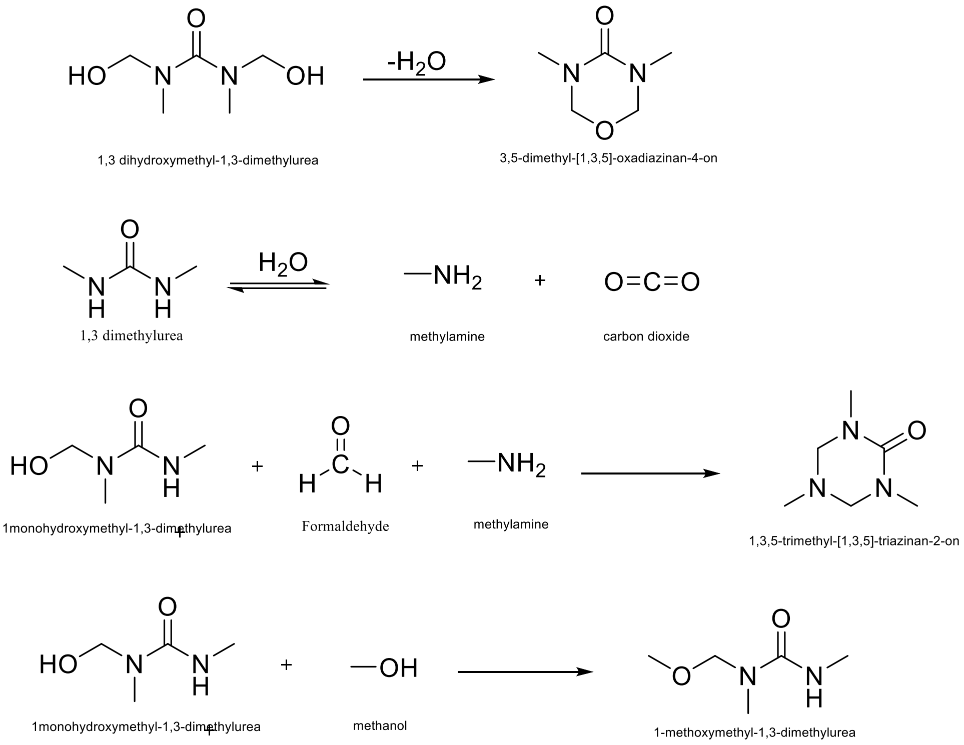

Figure 23. Side reactions of the hybrid UF reaction system

3.1.4 Preparation of Wood Composites

Three-layer laboratory-scale particleboards, each measuring 400 mm × 400 mm × 16 mm, were fabricated, comprising two surface layers and a central core layer. UF resin served as the adhesive, applied at a rate of 7 wt% for the surface layers and 11.5 wt% for the core layer, relative to the oven-dry weight of the wood particles. Before adhesive application, the wood particles were conditioned to a moisture content of approximately 4%. The mat structures were then manually formed and subjected to hot pressing at 200°C under a pressure of 100 bar for 5 min. The particleboards were produced with a target density of 640 kg/m^3.

3.1.5 Instruments

FTIR spectra were obtained using a ThermoScientific Nicolet iS50 FTIR spectrometer. ^{1}H-NMR analysis was carried out with a 60 MHz Benchtop spectrometer with DMSO-d_6 solvent. Thermogravimetric analysis (TGA) was conducted with the Mettler Toledo TGA 2 Star System instrument at a range of 25°C to 800°C with a 10°C/min heating rate and 20 ml/min nitrogen flow. Differential scanning calorimetry (DSC) analysis was performed with the Mettler Toledo DSC 3 Star System instrument with sample sizes of 8-10 mg. DSC thermograms were obtained with dynamic mode from 25°C to 300°C at a

10°C/min heating rate. All DSC studies were conducted under a nitrogen flow of 20 mL/min. The onset temperatures of thermal degradation were obtained where the tangent line at the inflection point of the DSC thermogram intersected with the baseline drawn at the point where the descent of the curve occurred. Viscosity measurements were conducted using a Brookfield DV2T viscometer with a SC4-2 1 type spindle. All samples were tested within the linear viscoelastic limit, and a 0.5 mm gap between the plates was maintained. The temperature sweep of the rheology test was conducted at temperatures from 25ºC to 200ºC with a linear 2ºC/min increment. To evaluate the gel time in the physical testing of the resin, 5 g of a 10% (w/w) aqueous ammonium chloride solution was added to 50 g of resin in a beaker. The mixture was stirred thoroughly until a homogeneous composition was obtained. A representative aliquot of the prepared mixture was then transferred into a test tube, into which a metal rod was placed. The test tube was subsequently immersed in a boiling water bath maintained at 100°C. At this point, a stopwatch was initiated. Stirring was continued manually with the metal rod, and the stopwatch was stopped at the onset of resin solidification. The elapsed time, recorded in seconds, was designated as the gel time. All pH measurements were performed using a Mettler Toledo pH meter. Before measurement, the electrode was immersed in the sample cooled to 20°C, and the pH value was recorded once it stabilized. The viscosity of the resin was measured using a Brookfield cap-cone type viscometer at 20°C. To measure the density of the resin, the resin was cooled to 20°C and kept in a 250 mL beaker. An appropriate hydrometer was carefully immersed in the sample, and the system was allowed to stabilize. Once the hydrometer reached equilibrium, the value indicated on the scale was recorded as the density of the resin, expressed in g/cm^3.To determine the solid content, a minimum of 1 g of resin sample was weighed into pre-weighed (tared) aluminum containers. For each sample, three replicates were prepared. The samples were then placed in a drying oven at 120°C for 2 hours. After the heating period, the containers were cooled to room temperature and reweighed. The solid content (%) was calculated using the following equation: Solid content% = (Weight after drying − Tare) × 100 / (Initial Weight − Tare). **Table 6** outlines the performance evaluation methods employed for wood composites.

3.2 Characterization of Alkyl Substituted Hybrid UF Resin

3.2.1 Structural Analysis of Hybrid Resin

3.2.1.1 FTIR

FTIR analysis was conducted to understand the structure of resins and to compare the hybrid resins with the reference UF. For all five resins, including the reference UF, the presence of hydroxyl groups (-OH) and water is observed as a broad absorption band in the range of 2900 cm^{-1} to 3650 cm^{-1} due to the strong hydrogen bonding effect. The stretching vibration observed at a range of 2955 cm^{-1} to 2962 cm^{-1} in all resins is attributed to sp^3-hybridized C–H stretching, which originates from sp^3-hybridized carbon and is partially obscured by the OH stretching. A strong peak appearing at a range of 985 cm^{-1} to 1003 cm^{-1} in all resins is due to C–O–C stretching vibrations. For 5% 1,3 DMUF, the corresponding peak is relatively weaker compared to other resins. All the resins exhibit weak signals at a range of 1247 cm^{-1} to 1258 cm^{-1} corresponding to CH_2 bending vibrations. A strong carbonyl (C=O) stretching band is observed due to changes in dipole moment, at a range of 1615 cm^{-1} to 1637 cm^{-1}. The N-H peak is observed at a range of 1537 cm^{-1} to 1539 cm^{-1}. All the resins show the same characteristic peaks at a very close range and are presented in **Figure 24**, and very minimal to no change is observed compared to the reference UF. However, 5% 1,3 DMUF resin shows less intensity compared to other resins.

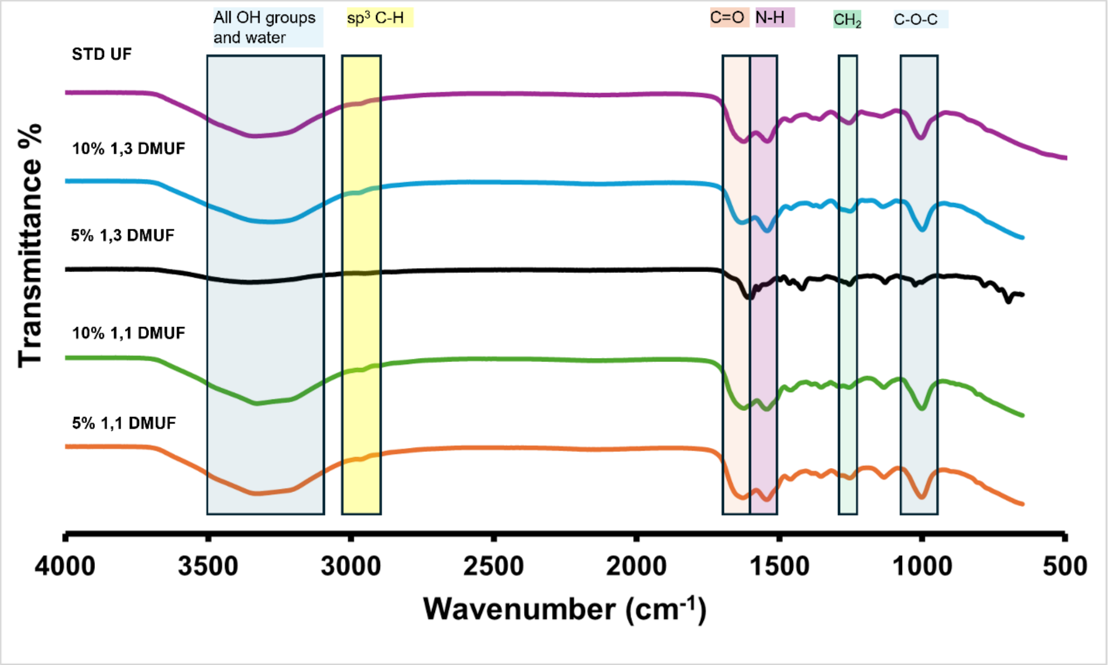

Figure 24. FTIR spectra of hybrid resins

3.2.1.2 NMR

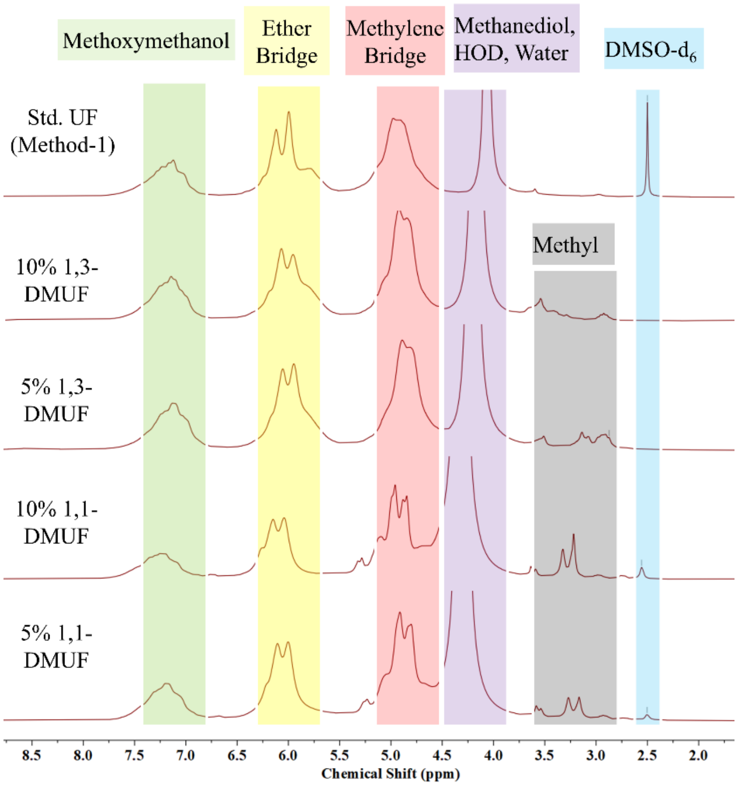

Figure 25. ^{1}H NMR data of hybrid resins

To gain deeper insight into the structural characteristics of hybrid resins, ^{1}H NMR spectroscopy was employed. As illustrated in **Figure 25**, chemical shifts corresponding to all protons associated with UF resin structures were detected, alongside identifiable peaks for DMSO-d6, water, and HOD. DMSO-d6, used both as solvent and external reference, exhibited a characteristic singlet at 2.5 ppm. The HOD and water signals appeared within the range of 3.5–4.1 ppm for reference UF and 5% 1,3-DMUF, 4.0 to 4.5 ppm for 1,1 DMUF. However, for 10% 1,3-DMUF, this peak has shifted to 5.0 to 5.5 ppm. Notably, methanediol (formaldehyde monohydrate or methylene glycol or oxymethylene glycol) resonates within the same region, resulting in a broad, composite peak with minor shoulder signals.

The NMR samples analyzed represent the final resin products, where the hydroxyl functionalities are expected to be substantially consumed. However, in all samples, methoxymethanol (hemiformal) signals are evident at different ranges. For the reference UF and 1,1-DMUF, this peak is found between 7.0 to 7.5 ppm, while 5% 1,3-DMUF shows at 6.5 to 7.0 and 10% 1,3-DMUF.

The characteristic resonance for amine protons (N–H) is typically observed around 9.0 ppm. However, such signals were not detected in any of the UF resin samples, likely due to limitations of the NMR instrument and hydrogen bonding effects, which can obscure N–H visibility in low-field spectra. High-field NMR instrumentation would be required for the reliable detection of these protons.

The primary objective of this NMR investigation was to identify and quantify the methylene and ether bridges, the two most critical crosslinking motifs in the UF network. The methylene bridge appeared within 4.5–5.5 ppm for the reference UF and 1,1-DMUF and shifted slightly to 4.0–5.0 ppm for 5% 1,3-DMUF. However, for 10% 1,3-DMUF, the methylene peak is found at 5.5 to 6.5 ppm. Similarly, ether bridges resonated at 5.5–6.5 ppm in the reference UF and 1,1 DMUF, shifting to 5.0–6.0 ppm in 5% 1,3DMUF. However, for 10% 1,3-DMUF, the ether peak is found at 6.5 to 7.5 ppm. The relative intensities of these peaks, derived via peak integration, offer a quantitative means to estimate the bridge ratio. Importantly, the methylene bridge is generally associated with increased hydrophobicity, whereas the ether bridge contributes to hydrophilicity. Therefore, this ^{1}H NMR analysis provides critical structural insights into the hydrophilic–hydrophobic balance of UF resins synthesized under varying reaction conditions, offering a valuable foundation for tailoring resin properties through synthetic control.

3.2.2 Thermal Stability and Curing of Hybrid Resin

3.2.2.1 TGA

Thermogravimetric analysis was conducted to assess the thermal stability and decomposition behavior of UF and MUF resins, with the results presented in **Figure 26**. The TGA profiles reveal that both resins exhibit a two-step degradation process: an initial mass loss attributed to the evaporation of water, followed by thermal decomposition of the polymer network. Approximately 50% weight loss was observed around 100°C for all resins, including the reference UF, indicating a high water content, consistent with the resins retaining roughly 50% water by weight due to the condensation reaction releasing water, and 37% formaldehyde solution is used in the reaction.

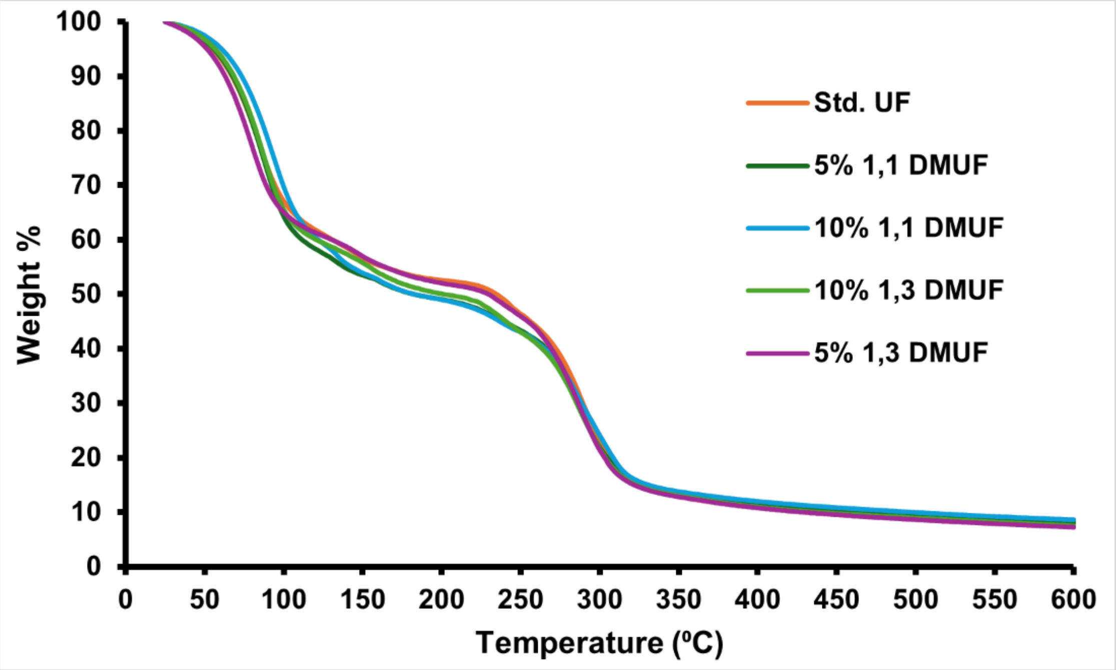

Figure 26. TGA of hybrid resins

As the temperature increased, substantial degradation of the resin matrix was evident. By 300°C, all the resins had lost nearly 80% of their initial mass. At 600°C, the cumulative mass loss reached approximately 80–90% for all resins. The char residue in all resins is the same in weight percentage. The TGA results revealed that incorporation of 1,1-DMU and 1,3-DMU does not change the thermal degradation and decomposition behavior. The same decomposition and degradation behavior was also observed for 5% and 10% incorporation of model compounds. Overall, all the hybrid resins synthesized in this study show the same decomposition and degradation behavior as the reference UF.

3.2.2.2 Dynamic DSC

To investigate the curing behavior of the reference UF and hybrid resins, dynamic DSC analysis was performed, as shown in **Figure 27**. Characterizing the curing behavior of all resins via DSC presents significant challenges, primarily due to the high water content inherent in these systems. The presence of water leads to fluctuations in the DSC thermal baseline, making it difficult to identify clear and reproducible curing peak temperatures. Although some studies attempt to eliminate water prior to DSC analysis to improve signal clarity, such approaches fail to accurately represent the in-situ curing behavior encountered in industrial applications, thereby resulting in curing profiles that lack practical relevance. An alternative and more representative method involves conducting DSC measurements using a pressurized pan system to minimize the interference from water evaporation. During heating, water evaporation near 100 °C produces a pronounced endothermic peak, which overlaps and partially masks the exothermic heat released during resin curing. Furthermore, the methylolation reaction is an endothermic process, which also contributes to the distortion of the exothermic curing peak. In addition, as the condensation reactions proceed over a wide temperature range from the onset of curing, the resulting water is continuously released and subsequently evaporated, producing additional endothermic effects. From the thermograms, it is evident that reference UF and 1,3-DMUF resins initiate curing at a lower temperature than 1,1-DMUF resin. This earlier onset, beginning around 95 °C for the reference UF and 1,3-DMUF resins compared to 1,3-DMUF at 110 °C, is attributed to the higher intrinsic reactivity of urea and 1,3-DMU over 1,1-DMU. A broad endothermic peak observed near 120°C in the 1,3-DMUF sample likely corresponds to water release and evaporation associated with condensation reactions. In contrast, a pronounced endothermic peak around 175°C in the 1,1-DMUF may be indicative of resin degradation.

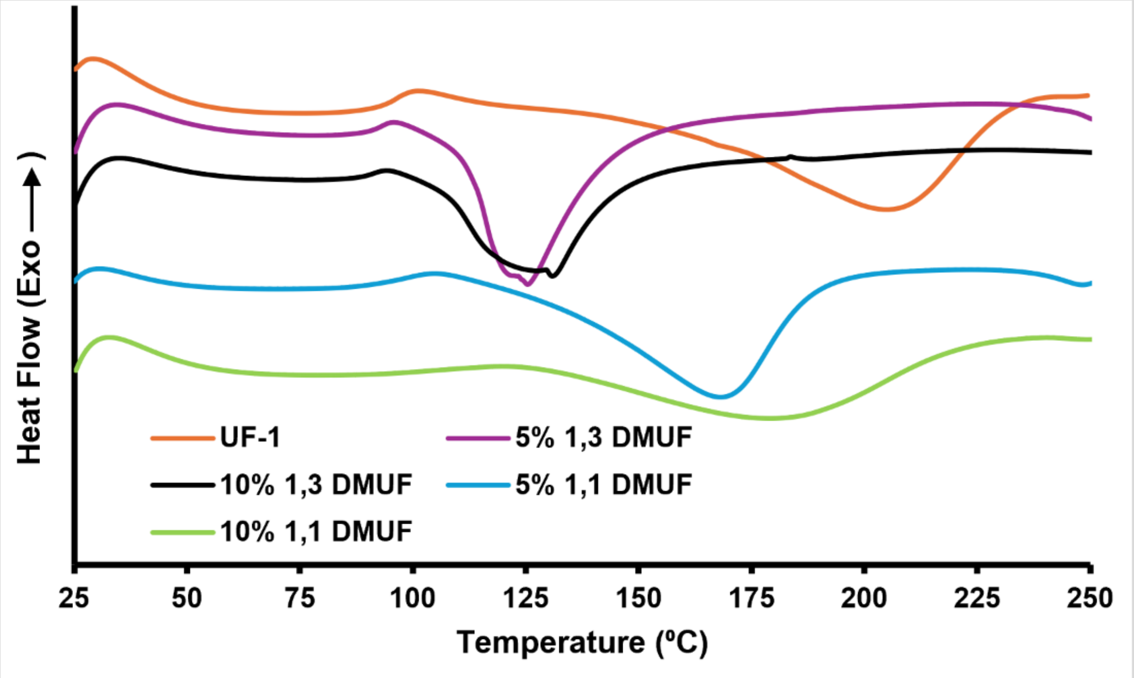

Figure 27. DSC Study of Hybrid Resin

It is critical to recognize that during the curing process of all resins, exothermic and endothermic processes occur concurrently. The dominant thermal event observed in the DSC thermogram is often the result of competing effects, where exothermic curing reactions are partially or fully offset by overlapping endothermic phenomena, such as water evaporation and methylolation.

3.2.3 Rheology of Hybrid Resin

To investigate the viscoelastic behavior of the reference UF and hybrid resins, a temperature sweep rheology test was conducted and presented in **Figure 28**. From the complex viscosity analysis of the resins, it is very clear that the reference UF starts curing earlier than other hybrid resins. 10% 1,1-DMUF takes the longest time and does not cure at all in the rheology test. 10% 1,3-DMUF also takes more time than others. However, unlike 10% 1,1-DMUF case, 10% 1,3-DMUF cures in the rheology test. 5% of both 1,1 and 1,3-DMUF takes more time to cure than the reference UF. Although the complex viscosity of 1,1-DMUF increases with the temperature, it does not cure completely.

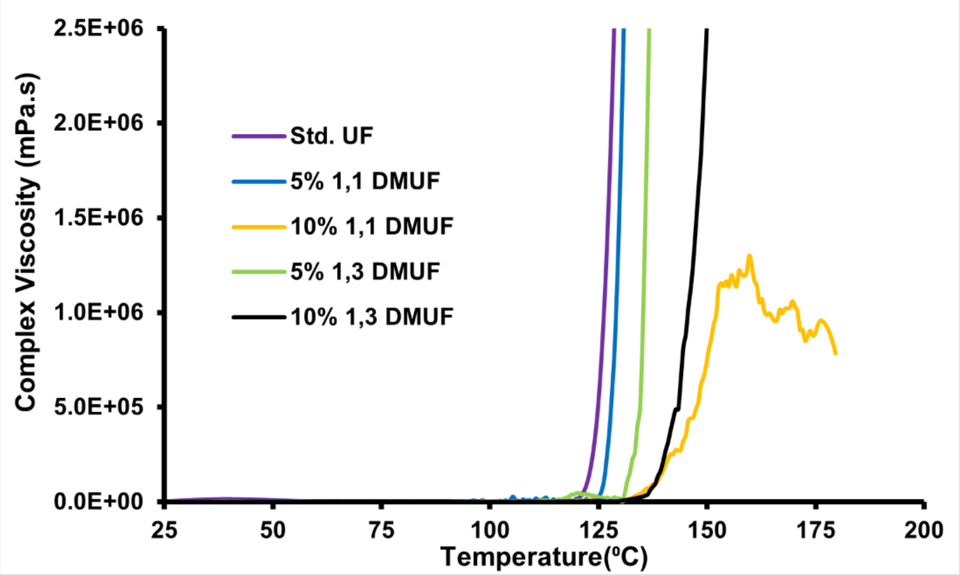

Figure 28. Rheology of hybrid resins

The onset of cure is around 120°C for the reference UF, 125°C for 5% 1,1-DMUF, 130°C for 5% 1,3-DMUF, and 135°C for both 10% 1,1-DMUF and 10% 1,1-DMUF. The expected curing of the reference UF starts earlier compared to the model system due to its higher reactivity and a higher number of substitutable amine protons compared to the dimethyl model compounds.

3.3 Understanding Physical Properties of Hybrid Resin

The physical properties of UF resins, including pH, viscosity, gel time, density, and solid content, were evaluated 24 h after the completion of resin synthesis. The results are summarized in **Table 4**. These parameters are critical for understanding resin formation mechanisms, processability, and performance in wood composite manufacturing. Moreover, they offer valuable insights into curing behavior, optimal hardener requirements, curing time, and the expected density, thickness, and overall quality of the resulting wood-based composites.

Table 4. Physical Properties of Hybrid Resin

Physical Properties of UF resin					
	Std. UF	5% 1,1 DMUF	10% 1,1 DMUF	5% 1,3 DMUF	10% 1,3 DMUF
pH	8.3	9.38	9.46	8.3	8.2
Viscosity mPa.s (20°C)	21	28	25	19	16
Gel time (s)	47	no gelation	no gelation	52	47
Density (g/cc)	1.214	1.208	1.21	1.215	1.215
Solid content (%)	54	47.06	50.24	52.73	51.85

The final pH of resins was adjusted to 8.5 for all resins without the use of buffering agents. However, pH measurements taken after 24 h indicated slight deviations, attributable to the continued condensation reactions occurring at ambient temperature. In some cases, such as 5% 1,1-DMUF and 10% 1,1-DMUF, a slight increase in pH was observed, which could result from ongoing methylolation reactions or urea decomposition under alkaline conditions, though such increases are relatively uncommon. Conversely, reference UF, 5% 1,3-DMUF, and 10% 1,3-DMUF showed a minor decrease in pH, likely due to hydrolysis of intermediate species, degradation of methylene bridges, or oxidation of residual formaldehyde. These small changes indicate reasonable room temperature stability of the synthesized resins. The viscosity values of the samples are relatively consistent with one another, and there was no substantial change in the viscosity over the 24 h.

The gel time of amino resin is defined by the time required to convert the liquid resin into a solid material at a specific temperature and conditions. This is one of the fundamental parameters that determine the quality of resin, curing behavior, and processing conditions. The gel time measurements revealed that formulations containing 5% 1,3-DMUF and 10% 1,3-DMUF exhibited gel times of 52 seconds and 47 seconds, respectively, and that is closely aligned with the standard UF resin benchmark (47 seconds). This similarity suggests that 1,3-DMUF-based formulations possess comparable crosslinking potential and network-forming capability to conventional UF resin. In contrast, the formulations incorporating 5% and 10% 1,1-DMUF exhibited no gelation under the test conditions.

This absence of gelation indicates a complete lack of crosslinking ability, confirming that 1,1-DMU is unsuitable as a reactive component in UF resin systems. As a result, these formulations are incapable of forming a three-dimensional polymer network and are therefore not viable for wood composites fabrication.

In general, an increase in gel time is associated with slower curing, which can adversely affect the mechanical performance of the final wood composite. Although longer gel times may offer improved storage stability, they often lead to higher formaldehyde emissions, extended curing durations, and decreased processing efficiency. Importantly, the absence of gelation entirely disqualifies a formulation from practical application in wood composite manufacturing.

As the F/U molar ratio and formaldehyde concentration (37%) were kept constant across all syntheses, minimal variation was observed in the density of the resins. All hybrid resins maintained a density close to 1.2 g/cm³, which is similar to the reference UF. A similar trend was observed in solid content measurements. Minor variations in solid content among the formulations were observed, such as 5% 1,1 DMUF having the lowest (47%), and the reference UF (54%) is the highest, primarily due to differences in the extent of condensation and water release during synthesis.

3.4 Methylene and Ether Bridge Formation in Hybrid Resin

To evaluate the hydrophobic and hydrophilic characteristics of the synthesized reference UF and hybrid resin, the relative proportions of methylene and ether bridges were quantified using ^{1}H NMR spectroscopy. The analysis considered the proton signals corresponding to methylene (-CH_2-) and ether (–CH_2–O–CH_2–) linkages. The raw integrated peak areas were obtained and subsequently normalized by dividing the area by 2 for methylene bridges and by 4 for ether bridges, corresponding to the number of protons contributing to each signal. The relative contributions of methylene and ether bridges within the polymer network were then estimated under the assumption that only these two types of linkages are formed during crosslinking (although 1,1-DMUF does not crosslink completely or does not form a network), excluding the possibility of the formation of cyclic structures. The percentage contributions of methylene and ether bridges are summarized in **Table 5**.

A general trend was observed from the data, indicating that incorporating the model compounds, either 1,1-DMU or 1,3-DMU, led to a higher methylene bridge ratio. This trend is evident in 5% 1,3-DMU and 10% 1,3-DMU, where the methylene bridge content increased by 17.94% and 25.45%, respectively, compared to the reference UF. Additionally, 5% 1,1-DMU and 10% 1,1-DMU also increased the methylene bridge by 24.73% and 26.31%, respectively. This may be due to the intrinsic attraction of methylol groups for the DMU compounds, or the presence of DMU may assist the reaction between methylol groups and urea, or the conversion of the ether bridge into a methylene bridge. However, the actual mechanism is currently unknown.

Table 5. Methylene and ether bridge calculation of hybrid resins

	Raw Integrated Area (Not Normalized)		Area Corresponding to Each proton		Ratio	Contribution to Structure (%)		Change in Methylene Bridge% (Compared to the Standard UF)
	Methylene Bridge	Ether Bridge	Methylene Bridge	Ether Bridge	Methylene to Ether Bridge	Methylene Bridge	Ether Bridge	
Standard UF	2.25	2.82	1.125	0.705	1.60	61.48	38.52	N/A
10% 1,1 DMUF	1.72	0.99	0.86	0.2475	3.47	77.65	22.35	26.31
10% 1,3 DMUF	3.22	1.91	1.61	0.4775	3.37	77.13	22.87	25.45
5% 1,1 DMUF	2.73	1.66	1.365	0.415	3.29	76.69	23.31	24.73
5% 1,3 DMUF	2.73	2.07	1.365	0.5175	2.64	72.51	27.49	17.94

3.5 Performance Analysis of Wood Composites (Produced with Hybrid Resin)

To evaluate the performance of the fabricated wood composites, a series of standardized tests were conducted, including internal bond (IB) strength, thickness swelling, water absorption, modulus of elasticity (MOE), modulus of rupture (MOR), and free formaldehyde content. The test results for wood composites prepared using the reference UF resin and hybrid resins are summarized in **Table 6**. The test standard is also provided in the same table.

Overall, 1,1 DMUF was found to be entirely ineffective for wood composite production. Physical testing clearly demonstrated that both 5% and 10% 1,1-DMUF formulations failed to undergo crosslinking under standard conditions, indicating an inability to form a polymer network without the application of extreme curing parameters. This lack of reactivity was further confirmed by the wood composite performance tests, in which all evaluated properties declined drastically. The mechanical performance was essentially negligible, with no meaningful bonding observed between wood particles. Additionally, thickness swelling and water absorption were excessively high, which is beyond the measurable range of the available instrumentation, further highlighting the absence of effective network formation. These findings conclusively demonstrate that 1,1-DMU is not a viable model compound for replacing urea in UF resin formulations and offers no functional performance in wood composite applications.

Table 6. Board test results of hybrid resins

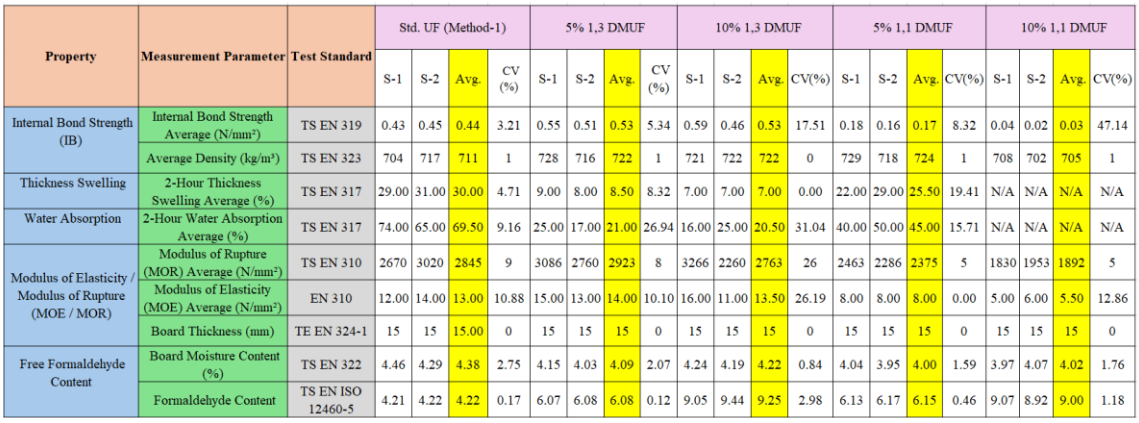

Property	Measurement Parameter	Test Standard	Std. UF (Method-1)				5% 1,3 DMUF				10% 1,3 DMUF				5% 1,1 DMUF				10% 1,1 DMUF			
			S-1	S-2	Avg.	CV (%)	S-1	S-2	Avg.	CV (%)	S-1	S-2	Avg.	CV(%)	S-1	S-2	Avg.	CV(%)	S-1	S-2	Avg.	CV(%)
Internal Bond Strength (IB)	Internal Bond Strength Average (N/mm²)	TS EN 319	0.43	0.45	0.44	3.21	0.55	0.51	0.53	5.34	0.59	0.46	0.53	17.51	0.18	0.16	0.17	8.32	0.04	0.02	0.03	47.14
	Average Density (kg/m³)	TS EN 323	704	717	711	1	728	716	722	1	721	722	722	0	729	718	724	1	708	702	705	1
Thickness Swelling	2-Hour Thickness Swelling Average (%)	TS EN 317	29.00	31.00	30.00	4.71	9.00	8.00	8.50	8.32	7.00	7.00	7.00	0.00	22.00	29.00	25.50	19.41	N/A	N/A	N/A	N/A
Water Absorption	2-Hour Water Absorption Average (%)	TS EN 317	74.00	65.00	69.50	9.16	25.00	17.00	21.00	26.94	16.00	25.00	20.50	31.04	40.00	50.00	45.00	15.71	N/A	N/A	N/A	N/A
Modulus of Elasticity / Modulus of Rupture (MOE / MOR)	Modulus of Rupture (MOR) Average (N/mm²)	TS EN 310	2670	3020	2845	9	3086	2760	2923	8	3266	2260	2763	26	2463	2286	2375	5	1830	1953	1892	5
	Modulus of Elasticity (MOE) Average (N/mm²)	EN 310	12.00	14.00	13.00	10.88	15.00	13.00	14.00	10.10	16.00	11.00	13.50	26.19	8.00	8.00	8.00	0.00	5.00	6.00	5.50	12.86
	Board Thickness (mm)	TE EN 324-1	15	15	15.00	0	15	15	15	0	15	15	15	0	15	15	15	0	15	15	15	0
Free Formaldehyde Content	Board Moisture Content (%)	TS EN 322	4.46	4.29	4.38	2.75	4.15	4.03	4.09	2.07	4.24	4.19	4.22	0.84	4.04	3.95	4.00	1.59	3.97	4.07	4.02	1.76
	Formaldehyde Content	TS EN ISO 12460-5	4.21	4.22	4.22	0.17	6.07	6.08	6.08	0.12	9.05	9.44	9.25	2.98	6.13	6.17	6.15	0.46	9.07	8.92	9.00	1.18

In contrast, resins synthesized with 1,3-DMUF demonstrated promising performance in the fabrication of wood composites, outperforming the standard UF resin in nearly all evaluated parameters, with the exception of formaldehyde emission. The elevated formaldehyde emissions observed in both 5% and 10% 1,3-DMUF formulations are likely due to the lower reactivity of 1,3-DMU compared to urea. This reduced reactivity may result in a minor fraction of unreacted formaldehyde remaining in the resin matrix, contributing to increased emissions.

Despite this limitation, 1,3-DMUF-based composites exhibited significantly improved internal bond (IB) strength, with a value of 0.53 N/mm² compared to 0.44 N/mm² for the standard UF resin. Additionally, dramatic improvements were observed in both thickness swelling and water absorption, attributable to the higher methylene bridge content, which enhances the hydrophobic character of the resin network. For example, the thickness swelling was reduced to 8.50% and 7.00% for 5% and 10% 1,3-DMUF formulations, respectively, compared to 30.0% for the standard UF. Similarly, water absorption decreased to 21.0% and 20.5% for 5% and 10% 1,3-DMUF, respectively, in contrast to 69.5% for the standard UF resin.

In terms of modulus of rupture (MOR), modulus of elasticity (MOE), and board moisture content, all three resin systems displayed comparable performance. The board thickness was also consistent across all samples, indicating uniformity in fabrication conditions.

Finally, 1,3-DMUF-based resins significantly enhance wood composite performance, demonstrating 3 to 4 times improvement in key properties such as dimensional stability and bonding strength, while maintaining parity in mechanical properties. The primary drawback remains the higher formaldehyde emission, which warrants further formulation optimization.

4 Conclusions

In this study, two distinct strategies were employed to enhance the hydrophobicity of urea-formaldehyde (UF) resins to improve wood composites' performance: (i) modification of synthesis parameters, and (ii) incorporation of alkyl-substituted urea model compounds into the resin formulation.

The first approach focused on increasing the methylene bridge content relative to ether bridges, as this structural feature is known to enhance hydrophobicity. A well-established industrial UF resin synthesis method was selected as the reference, and seven modified formulations were developed. In Method 2, increasing the reaction temperature from 80 °C to 98 °C and decreasing the pH from 5.5 to 5.0 led to a 15.6% increase in methylene bridge content. Method 3 introduced the gradual addition of urea over 30 min, resulting in negligible change. Method 4 altered the sequence of reactant addition, which yielded a 7.3% increase. In Method 5, combining a higher temperature with the reverse addition order significantly increased the methylene bridge content by 26.5%. Extending the formaldehyde addition time to 2 hours (Method 6) and 3 h (Method 7) further increased the methylene bridge content to 27.4% and 27.9%, respectively.

While the enhanced hydrophobicity improved moisture resistance, it also introduced compatibility issues with the hydrophilic wood particles. As a result, certain formulations, such as Methods 7 and 8, exhibited poor internal bond strength. Nevertheless, Method 5-based wood composites demonstrated superior overall performance across most measured properties, with the exception of formaldehyde emission. Notably, Methods 7 and 8 reduced formaldehyde emission by approximately threefold compared to the reference method and showed favorable results in terms of moisture content, modulus of rupture (MOR), and modulus of elasticity (MOE). However, the poor mechanical strength due to resin and wood incompatibility remains a major challenge.

The second strategy involved modifying the resin by incorporating 1,3-DMU and 1,1-DMU at different percentages as model compounds. The 1,1-DMUF formulations proved entirely unsuitable for wood composite fabrication due to their inability to form a crosslinked polymer network. No gelation was observed for either the 5% or 10% 1,1-DMUF formulations, confirming their lack of capability of forming a 3D polymer network structure.

In contrast, 1,3-DMUF resins (both 5% and 10%) showed promising results in nearly all performance metrics, with the exception of formaldehyde emission. These formulations exhibited enhanced dimensional stability, with significant reductions in thickness swelling and water absorption due to increased methylene bridge formation. Internal bond strength was also higher than that of the standard UF resin.

Although both Method 5 and 1,3-DMUF formulations offer considerable improvements in critical performance areas, higher formaldehyde emissions remain a major limitation for large-scale application. Future research should focus on strategies to suppress formaldehyde release, potentially through the incorporation of formaldehyde scavengers that can consume unreacted formaldehyde even in the presence of lower percentages, fillers, or co-additives. Meanwhile, although Methods 7 and 8 successfully reduce formaldehyde emission, their poor compatibility with wood particles limits their mechanical performance. Addressing this issue may require the development of compatibilizers or surface modification techniques to improve interfacial adhesion between the hydrophobic resin and hydrophilic wood substrates.

References

1. Pizzi, A. and K. Mittal, *Urea-formaldehyde adhesives.* Handbook of adhesive technology, 2003. **2**.
2. Dunky, M., *Urea–formaldehyde (UF) adhesive resins for wood.* International Journal of Adhesion and Adhesives, 1998. **18**(2): p. 95-107.
3. Khan, T.A., et al., *Synthesis of micro carbonaceous material by pyrolysis of rubber wood and its effect on properties of urea-formaldehyde (UF) resin.* International Journal of Adhesion and Adhesives, 2020. **99**: p. 102589.
4. Tollens, B., *I. Ueber einige Derivate des Formaldehyds.* Berichte der deutschen chemischen Gesellschaft, 1884. **17**(1): p. 653-659.
5. Rammon, R.M., et al., *The chemical structure of UF resins.* The Journal of Adhesion, 1986. **19**(2): p. 115-135.
6. Hanns, J., *Manufacture of aldehyde condensation product capable of technical utilization*. 1920, Google Patents.
7. Goldschmidt, C., *Ueber die Einwirkung von Formaldehyd auf Harnstoff.* Berichte der deutschen chemischen Gesellschaft, 1896. **29**(3): p. 2438-2439.
8. Wibowo, E.S., B.-D. Park, and V. Causin, *Recent advances in urea–formaldehyde resins: converting crystalline thermosetting polymers back to amorphous ones.* Polymer Reviews, 2022. **62**(4): p. 722-756.
9. Kibrik, É.J., et al., *On-line NMR spectroscopic reaction kinetic study of urea–formaldehyde resin synthesis.* Industrial & Engineering Chemistry Research, 2014. **53**(32): p. 12602-12613.
10. Pizzi, A. and K.L. Mittal, *Wood adhesives*. 2010: VSP Rancho Cordova, CA, USA.
11. Maloney, T.M., *The family of wood composite materials.* Forest products journal, 1996. **46**(2): p. 18.
12. Schneider, M. and A. Witt, *History of wood polymer composite commercialization.* Forest products journal, 2004. **54**(4): p. 19.
13. Smith, P.M. and M.P. Wolcott, *Opportunities for Wood/Natural Fiber-Plastic Composites in Residential and Industrial Applications.* Forest Products Journal, 2006. **56**(3).
14. Clemons, C.M. *Woodfiber-plastic composites in the United States–History and current and future markets*. in *Proceedings of the 3rd International Wood and Natural Fiber Composites Symposium*. 2000.
15. Khan, M.Z., S.K. Srivastava, and M. Gupta, *A state-of-the-art review on particulate wood polymer composites: Processing, properties and applications.* Polymer Testing, 2020. **89**: p. 106721.
16. BARBU, M.C., *Evolution of lightweight wood composites.* Pro Ligno, 2015. **11**(4).
17. Barbu, M. *An overview of the forestry and wood industry development worldwide*. in *Proceeding of the 26th International Conference on Wood Science and Technology*. 2015.
18. Sandberg, D., *Additives in wood products—today and future development*, in *Environmental impacts of traditional and innovative forest-based Bioproducts*. 2016, Springer. p. 105-172.

19. Mantanis, G.I., et al., *Adhesive systems used in the European particleboard, MDF and OSB industries.* Wood material science & engineering, 2018. **13**(2): p. 104-116.
20. Athanassiadou, E., C. Markessini, and S. Tsiantzi. *Industrial amino adhesives satisfying stringent formaldehyde limits*. in *2015 Melamine Conference*. 2015.
21. Vnučec, D., A. Kutnar, and A. Goršek, *Soy-based adhesives for wood-bonding–a review.* Journal of Adhesion Science and Technology, 2017. **31**(8): p. 910-931.
22. Hemmilä, V., et al., *Development of sustainable bio-adhesives for engineered wood panels–A Review.* Rsc Advances, 2017. **7**(61): p. 38604-38630.
23. Nakos, P., et al. *Environmentally-friendly adhesives for wood products used in construction applications*. in *Proc. of WCTE 2016-World Conference on Timber Engineering*. 2016.
24. Ramesh, M., et al., *A critical review on wood-based polymer composites: Processing, properties, and prospects.* Polymers, 2022. **14**(3): p. 589.
25. Kamps, J.J., et al., *How formaldehyde reacts with amino acids.* Communications Chemistry, 2019. **2**(1): p. 126.
26. Hoffman, E.A., et al., *Formaldehyde crosslinking: a tool for the study of chromatin complexes.* Journal of Biological Chemistry, 2015. **290**(44): p. 26404-26411.
27. Thorn, D., *The coordination chemistry of formaldehyde.* Journal of Molecular Catalysis, 1982. **17**(2-3): p. 279-288.
28. Humans, I.W.G.o.t.E.o.C.R.t., *Wood dust and formaldehyde.* 1995.
29. Lupieri, P., et al., *Spectroscopic Properties of Formaldehyde in Aqueous Solution: Insights from Car− Parrinello and TDDFT/CASPT2 Calculations.* Journal of chemical theory and computation, 2010. **6**(11): p. 3403-3409.
30. Albert, M., et al., *Vapor-liquid and chemical equilibria of formaldehyde-water mixtures.* AIChE journal, 1999. **45**(9): p. 2024-2033.
31. Bernardini, L., et al., *Formaldehyde toxicity reports from in vitro and in vivo studies: a review and updated data.* Drug and chemical toxicology, 2022. **45**(3): p. 972-984.
32. Godfrey, P.D., R.D. Brown, and A.N. Hunter, *The shape of urea.* Journal of molecular structure, 1997. **413**: p. 405-414.
33. Wöhler, F., *Ueber künstliche bildung des harnstoffs.* Annalen der Physik, 1828. **88**(2): p. 253-256.
34. Volz, N. and J. Clayden, *The urea renaissance.* Angewandte Chemie International Edition, 2011. **50**(51): p. 12148-12155.
35. Kapuscinska, A. and I. Nowak, *The use of urea and its derivatives in the cosmetics industry.* Chemik, 2014. **68**(2): p. 91-98.
36. Ghosh, A.K. and M. Brindisi, *Urea derivatives in modern drug discovery and medicinal chemistry.* Journal of medicinal chemistry, 2019. **63**(6): p. 2751-2788.
37. Mavrovic, I. and A.R. Shirley Jr, *GR "Buck" Coleman, Urea.* Kirk-Othmer Encyclopedia of Chemical Technology: p. 1-21.
38. Chen, C., et al., *Coupling N2 and CO2 in H2O to synthesize urea under ambient conditions.* Nature chemistry, 2020. **12**(8): p. 717-724.
39. Koltzenburg, S., M. Maskos, and O. Nuyken, *Polymer chemistry*. 2017: Springer.

40. Kumar, R.N., et al., *Studies in the process optimization and characterization of low formaldehyde emission urea-formaldehyde resin by response surface methodology.* Journal of Applied Polymer Science, 2007. **103**(4): p. 2709-2719.
41. Ebdon, J. and P. Heaton, *Characterization of urea-formaldehyde adducts and resins by 13C-nmr spectroscopy.* Polymer, 1977. **18**(9): p. 971-974.
42. Tomita, B. and H. Ono, *Melamine–formaldehyde resins: Constitutional characterization by fourier transform 13C-NMR spectroscopy.* Journal of Polymer Science: Polymer Chemistry Edition, 1979. **17**(10): p. 3205-3215.
43. Li, T.H., et al., *A computational exploration of the mechanisms for the acid-catalytic urea–formaldehyde reaction: new insight into the old topic.* Journal of Physical Organic Chemistry, 2012. **25**(2): p. 118-125.
44. Smets, G. and A. Borzee, *Réactions de condensation de formaldéhyde et d'urée.* Journal of polymer science, 1952. **8**(4): p. 371-394.
45. Smythe, L.E., *A Kinetic Study of the Urea–Formaldehyde Reaction.* The Journal of Physical Chemistry, 1947. **51**(2): p. 369-378.
46. Pizzi, A. and C. Ibeh, *Aminos*, in *Handbook of thermoset plastics*. 2014, Elsevier. p. 75-91.
47. Shenai, V. and J. Manjeshwar, *Kinetics of the reaction between urea and formaldehyde in the presence of sulfuric acid.* Journal of Applied Polymer Science, 1974. **18**(5): p. 1407-1410.
48. De Jong, J. and J. De Jonge, *The chemical composition of some condensates of urea and formaldehyde.* Recueil des Travaux Chimiques des Pays-Bas, 1953. **72**(12): p. 1027-1036.
49. Glutz, B. and H. Zollinger, *Allgemeine Säure-Basen-Katalyse der Monomethylol-Bildung aus Harnstoff und Formaldehyd in Wasser.* Helvetica Chimica Acta, 1969. **52**(7): p. 1976-1984.
50. Li, T., et al., *Re-elucidation of the acid-catalyzed urea–formaldehyde reactions: A theoretical and 13C-NMR study.* Journal of Applied Polymer Science, 2016. **133**(48).
51. Nair, B.R. and D.J. Francis, *Kinetics and mechanism of urea-formaldehyde reaction.* Polymer, 1983. **24**(5): p. 626-630.
52. Sun, Q.N., C.Y. Hse, and T.F. Shupe, *Effect of different catalysts on urea–formaldehyde resin synthesis.* Journal of Applied Polymer Science, 2014. **131**(16).
53. De Jong, J. and J. De Jonge, *The hydrolysis of methylene diurea.* Recueil des Travaux Chimiques des Pays-Bas, 1953. **72**(3): p. 202-206.
54. Despres, A., et al., *Comparative 13C-NMR and matrix-assisted laser desorption/ionization time-of-flight analyses of species variation and structure maintenance during melamine–urea–formaldehyde resin preparation.* Journal of applied polymer science, 2007. **106**(2): p. 1106-1128.
55. Kumar, A. and V. Katiyar, *Modeling and experimental investigation of melamine-formaldehyde polymerization.* Macromolecules, 1990. **23**(16): p. 3729-3736.
56. Tomita, B., *Melamine–formaldehyde resins: Molecular species distributions of methylolmelamines and some kinetics of methylolation.* Journal of Polymer Science: Polymer Chemistry Edition, 1977. **15**(10): p. 2347-2365.
57. Odian, G., *Principles of polymerization*. 2004: John Wiley & Sons.
58. Humans, I.W.G.o.t.E.o.C.R.t., *Formaldehyde*, in *Wood Dust and Formaldehyde*. 1995, International Agency for Research on Cancer.

59. Paiva, N.T., et al., *Production of melamine fortified urea-formaldehyde resins with low formaldehyde emission.* Journal of Applied Polymer Science, 2012. **124**(3): p. 2311-2317.
60. Daily, K.A., et al., *Formaldehyde exposure in nonoccupational environments.* Archives of Environmental Health: An International Journal, 1981. **36**(6): p. 277-284.
61. Salthammer, T., S. Mentese, and R. Marutzky, *Formaldehyde in the indoor environment.* Chemical reviews, 2010. **110**(4): p. 2536-2572.
62. Octavia, Z. *Standards and regulations concerning the formaldehyde emissions from wood panels*. in *13th ınternatıonal conference "Standardızatıon, Protypes And Qualıty: A Means Of Balkan Countrıes' Collaboratıon" Brasov, Romania, November*. 2016.
63. Ohalete, M. and A. Popoola, *Urea-formaldehyde resins synthesis, modification and characterization.* IOSR J. Appl. Chem, 2019. **12**: p. 19-25.
64. Wang, B., et al., *Melamine-urea-formaldehyde resins with low formaldehyde emission and resistance to boiling water.* Pigment & Resin Technology, 2019. **48**(3): p. 229-236.
65. Jiang, S., et al., *Highly branched polyurea-enhanced urea-formaldehyde resin.* ACS Applied Polymer Materials, 2021. **3**(2): p. 1157-1170.
66. Peng, J., et al., *Characterization on the copolymerization resin between bayberry (Myrica rubra) tannin and pre-polymers of conventional urea–formaldehyde resin.* Forests, 2022. **13**(4): p. 624.
67. Pang, J.Y., et al., *Study on modification of urea formaldehyde resin with keratin.* Advanced Materials Research, 2010. **113**: p. 1787-1791.
68. Hong, W., et al., *Thermal analysis study of modified urea-formaldehyde resin.* 폴리머, 2016. **40**(5): p. 707-713.
69. Wibowo, E.S., M.A.R. Lubis, and B.-D. Park, *In-situ modification of low molar ratio urea–formaldehyde resins with cellulose nanofibrils for plywood.* Journal of Adhesion Science and Technology, 2021. **35**(22): p. 2452-2465.
70. Ebewele, R.O., et al., *Polyamine-modified urea-formaldehyde resins. I. Synthesis, structure, and properties.* Journal of Applied Polymer Science, 1991. **42**(11): p. 2997-3012.
71. Heinrich, L.A., *Future opportunities for bio-based adhesives–advantages beyond renewability.* Green chemistry, 2019. **21**(8): p. 1866-1888.
72. Steinhof, O., G. Scherr, and H. Hasse, *Investigation of the reaction of 1, 3-dimethylurea with formaldehyde by quantitative on-line NMR spectroscopy: a model for the urea–formaldehyde system.* Magnetic Resonance in Chemistry, 2016. **54**(6): p. 457-476.